CHEMICAL REVIEWS

Review

Cite This: Chem. Rev. XXXX, XXX, XXX−XXX

pubs.acs.org/CR

# Paranemic Crossover DNA: There and Back Again

Xing Wang,[*,†] Arun Richard Chandrasekaran,[*,‡] Zhiyong Shen,[§] Yoel P. Ohayon,[∥] Tong Wang,[∥] Megan E. Kizer,[†] Ruojie Sha,[∥] Chengde Mao,[⊥] Hao Yan,[#] Xiaoping Zhang,[∥] Shiping Liao,[∥] Baoquan Ding,[∥] Banani Chakraborty,[∥] Natasha Jonoska,[▽] Dong Niu,[∥] Hongzhou Gu,[∥] Jie Chao,[∥] Xiang Gao,[∥] Yuhang Li,[∥] Tanashaya Ciengshin,[∥] and Nadrian C. Seeman[*,∥]

[†]Department of Chemistry and Chemical Biology and The Center for Biotechnology and Interdisciplinary Studies, Rensselaer Polytechnic Institute, Troy, New York 12180, United States

[‡]Confer Health, Incorporated, Charlestown, Massachusetts 02129, United States

[§]College of Chemistry and Materials Science, Anhui Normal University, Wuhu, Anhui 241000, China

[∥]Department of Chemistry, New York University, New York, New York 10012, United States

[⊥]Department of Chemistry, Purdue University, West Lafayette, Indiana 47907, United States

[#]Department of Chemistry and Biochemistry and The Biodesign Institute, Arizona State University, Tempe, Arizona 85287, United States

[▽]Department of Mathematics and Statistics, University of South Florida, Tampa, Florida 33620, United States;

**ABSTRACT:** Over the past 35 years, DNA has been used to produce various nanometer-scale constructs, nanomechanical devices, and walkers. Construction of complex DNA nanostructures relies on the creation of rigid DNA motifs. Paranemic crossover (PX) DNA is one such motif that has played many roles in DNA nanotechnology. Specifically, PX cohesion has been used to connect topologically closed molecules, to assemble a three-dimensional object, and to create two-dimensional DNA crystals. Additionally, a sequence-dependent nanodevice based on conformational change between PX and its topoisomer, $JX_2$, has been used in robust nanoscale assembly lines, as a key component in a DNA transducer, and to dictate polymer assembly. Furthermore, the PX motif has recently found a new role directly in basic biology, by possibly serving as the molecular structure for double-stranded DNA homology recognition, a prominent feature of molecular biology and essential for many crucial biological processes. This review discusses the many attributes and usages of PX-DNA—its design, characteristics, applications, and potential biological relevance—and aims to accelerate the understanding of PX-DNA motif in its many roles and manifestations.

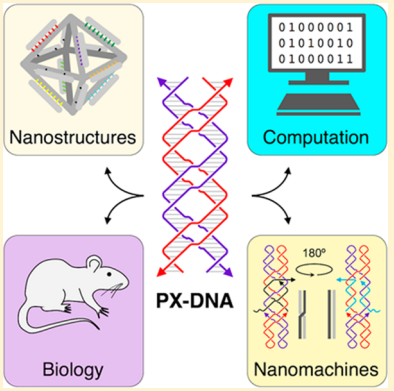


## CONTENTS



**Special Issue:** Nucleic Acid Nanotechnology

**Received:** March 31, 2018






DOI: 10.1021/acs.chemrev.8b00207
Chem. Rev. XXXX, XXX, XXX−XXX

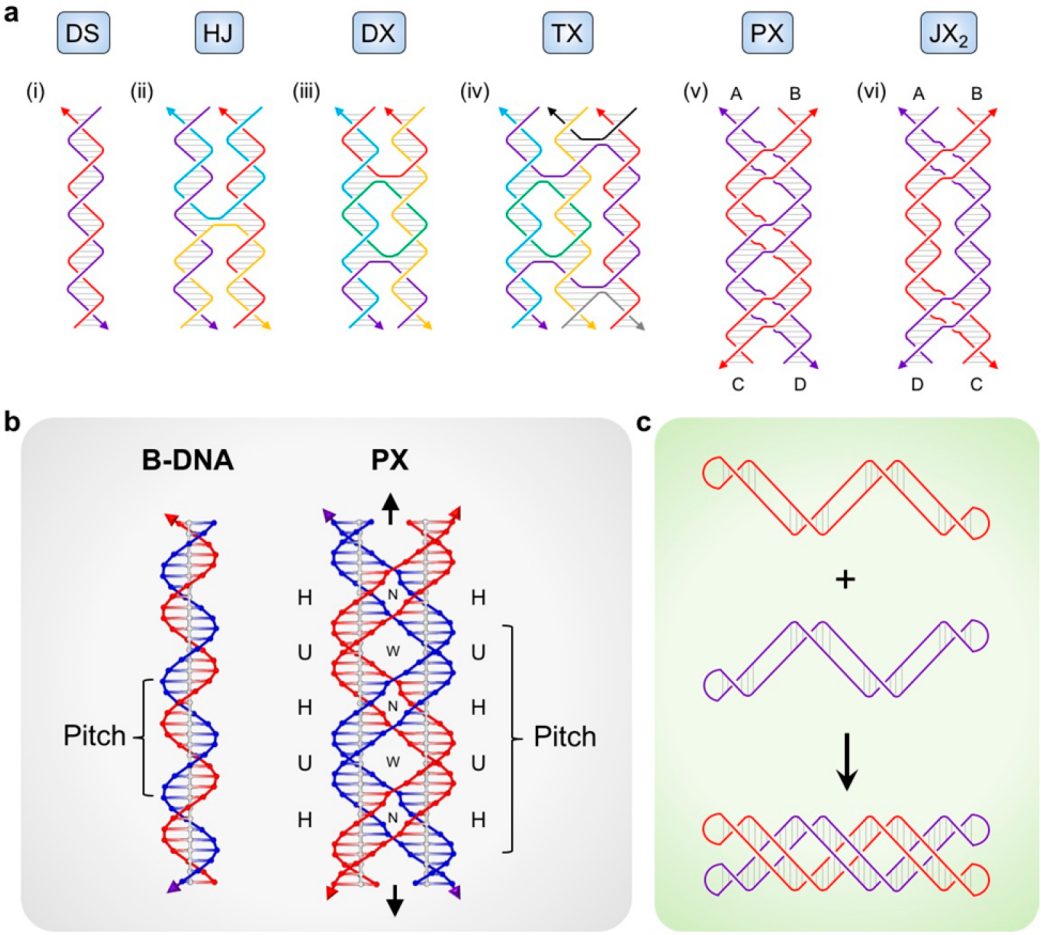


**Figure 1.** Design of DNA motifs. (a) Motifs used in DNA nanotechnology: (i) Double-stranded DNA (DS). (ii) Holliday junction (HJ), a four-arm junction that results from a single reciprocal exchange between double helices. (iii) Double-crossover (DX) molecule resulting from a double reciprocal exchange between double helices. (iv) Triple-crossover (TX) molecule that results from two successive double reciprocal exchanges involving three helical domains. Note that HJ, DX, and TX molecules all contain reciprocal exchanges between strands of opposite polarity. (v) Paranemic crossover (PX) DNA, where two double helices exchange strands at every possible point where the helices come into proximity. (vi) $JX_2$ molecule, a topoisomer of PX, that lacks two crossovers in the middle in contrast to the PX molecule. The orientation of the bottom helical segments of PX and $JX_2$ molecules differ by a half-turn of DNA (about 180°) as denoted by alphabetic labels. Note that exchanges in the PX and $JX_2$ molecules are between strands of the same polarity. (b) Comparison of B-DNA and PX-DNA. PX-DNA consists of interwrapped blue and red double helices. Black arrowheads indicate the dyad axis of the molecule. For any given half-turn of DNA, either a major (wide) groove separation (indicated by W) or a minor (narrow) groove separation (indicated by N) can flank the dyad axis. The helical pitches of both structures are indicated. Half turns labeled U do not require complementarity between the blue and red strands for the PX structure to form, but those labeled H do require it, so the sequences must be homologous in those regions.[24] (c) Paranemic cohesion. Two half-PX molecules (closed dumbbells) are partly complementary within the same strand and have PX complementarity to the other half-PX molecule. The two halves can interweave to cohere two topologically closed molecules.[40]



## 1. INTRODUCTION

DNA, known as the hereditary material in almost all organisms, has been used since the 1980s[1] as a building block for the directed self-assembly of custom two- and three-dimensional (2D and 3D) objects, arrays, and devices bearing features on the nanometer scale.[2,3] The suitability of DNA for this purpose is rooted in its inherent nanoscale features (diameter ∼2 nm, helical pitch ∼3.5 nm, and persistence length ∼50 nm), its predictable intermolecular strand recognition (where adenine pairs with thymine and guanine pairs with cytosine), and its programmable nature (the base sequence and oligonucleotide length). DNA-based nanoscale construction relies on stable motifs. Paranemic crossover (PX) DNA[4] is a unique four-stranded coaxial DNA motif. It contains a group of DNA complexes with different major-groove separations and has introduced a novel and unprecedented paradigm in DNA nanotechnology by serving as a central element for manufacturing state-of-the-art and programmable nanomechanical devices,[5−11] including an assembly line[12] and a DNA computing system.[13,14] It has also been used for synthesizing nanostructures that span the range from individual objects[15,16]


DOI: 10.1021/acs.chemrev.8b00207
Chem. Rev. XXXX, XXX, XXX−XXX

to one-dimensional (1D)[17−19] and 2D periodic arrays.[20,21] PX-DNA is a molecule that bridges DNA nanotechnology and biology and is the first designer/complex DNA motif that has been successfully replicated in vitro[22] and in vivo,[23] by use of naturally existing protein machinery. Beyond its contribution as a molecular building block to DNA nanotechnology and DNA computing, the PX-DNA motif has recently found a potential new role directly in basic biology, by possibly serving as the molecular structure for double-stranded DNA homology recognition,[24] a prominent feature of molecular biology and essential for many crucial biological processes. The PX motif has been one of the major contributors to the research of DNA nanotechnology since the first PX-based paper[5] was published in *Nature* in 2002.

In this review, we discuss characteristics of the PX-DNA motif and efforts to use this motif in nanomechanical devices, 1D and 2D arrays, DNA computing, and DNA-based objects, as well as its implied role in biology, which will cover the literature published from 1964 to now. As the PX-DNA motif has entered a new era of importance in chemistry, materials science, and biology, we highlight the directions of PX-oriented research to shed light on future uses of the PX-DNA motif to create functional DNA nanomaterials and nanodevices, both in vitro and in vivo, and to point out how this synthetic molecular tool may help to elucidate the underlying mechanism for highly complex double-stranded DNA homology recognition, which will have broad implications for basic biology.

## 2. DESIGNER DNA MOTIFS AND PARANEMIC CROSSOVER DNA

The DNA double helix is mostly a topologically linear chain [Figure 1a(i)], and connecting many such linear molecules would mainly result in a longer linear (1D) structure. For it to be used in constructing structures that span multiple dimensions, a branch point is required. Branched DNA molecules can be created by crossover (i.e., by reciprocal exchange) of strands between two adjacent double helices. Such branched DNA junctions are known to occur in nature, such as the Holliday junction (HJ) [Figure 1a(ii) illustrates a singly branched HJ] that is known to be an intermediate in genetic recombination.[25] However, naturally occurring branched DNA junctions are not stable, and the junction points can migrate via branch recombination due to 2-fold sequence symmetry. Immobile DNA junctions have been created by a sequence symmetry minimization strategy,[1,26] made possible by the chemical synthesis of DNA strands with any desired sequence. Branched DNA junctions containing three, four, five, six, eight, or 12 DNA double-helix arms have been assembled and characterized.[26−29] Furthermore, rigid DNA motifs have been designed and constructed by performing multiple reciprocal exchanges between strands of the same or opposite polarity. Two early examples of such rigid and stable DNA motifs are the double-crossover [DX, containing two DNA duplexes; Figure 1a(iii)][30] and triple-crossover [TX, containing three DNA duplexes; Figure 1a(iv)][31] structures, derived by reciprocal exchange between strands of either the same polarity, opposite polarity, or a combination of both. These two rigid DNA motifs have been further assembled into periodic DNA 2D arrays[31,32] that have successfully served as molecular platforms to arrange external elements, such as gold nanoparticles[33] or peptides,[34] with nanometer precision.

### 2.1. Characteristics of Paranemic Crossover DNA

Paranemic crossover (PX) DNA is a four-stranded DNA structure that is created by reciprocal exchange between strands of the same polarity at every possible point where two juxtaposed DNA duplexes come in close proximity. It has a paranemic character because the backbones of the two component helices, as shown in Figure 1a(v) and Figure 1b, are not linked and thus can be separated from each other without the need for strand scission. In comparison to B-DNA (Figure 1b), the helical repeat of two individual DNA domains (red or blue) in the PX structure is similar to the twist in canonical B-form DNA duplex. However, the helical repeat of PX-DNA is about twice that of conventional B-DNA; that is, the net twist is about half that of B-DNA. For any given half-turn of PX-DNA, a major (wide) groove separation (denoted by W) or a minor (narrow) groove separation (denoted by N) can flank the central dyad axis of the structure. PX complexes with a major-groove separation of five, six, seven, eight, or nine nucleotide pairs and a minor-groove separation of four, five, or six nucleotide pairs have been successfully assembled (denoted PX-5:5, 6:4, 6:5, 6:6, 7:4, 7:5, 8:5, and 9:5, corresponding to the number of nucleotides in the major and minor grooves, respectively).[4] Such PX motifs have been proved to be stable in solution by both molecular dynamics (MD) simulations and experiments.[4,35] PX complexes with major/minor-groove separations such as 5:5, 6:4, and 7:4 have been recently used to assemble DNA objects and 2D arrays.[15,20] Additionally, the PX structure can be assembled from a simple topologically closed single-stranded DNA, which lays the basis for PX amplification by use of biological machinery.[22,23] Furthermore, a topoisomer of PX structure, $JX_2$, that lacks two crossovers [Figure 1a(vi)] and thereby differs from PX structure by a half DNA turn rotation [about a 180° rotation of the bottom helices, denoted by the letters flanking their helices in Figure 1a(v,vi)], has been designed and used as a key motor component for operating various sequence-dependent DNA nanomechanical devices/machines.[5−7,9,12]

As illustrated in Figure 1b, formation of a PX molecule can also be viewed as the interwrapping of two double-stranded DNAs, one pair red and one pair blue. Along the two DNA duplexes in PX, intrahelix base pairing is indicated as alternating between two paired red strands or two paired blue strands (in the half turns labeled U), and interhelix base pairing is formed between paired red and blue strands (in the half turns labeled H). Essentially, the regions denoted U do not require complementarity, while homology is needed only in the half turns labeled H to form PX-DNA if the sequences are not designed to minimize sequence symmetry. Hence, two DNA double helices are so-called PX-homologous if they contain identical sequences in the half-turns labeled H but not in the half-turns labeled U. Of course, the ability of two double helices that carry PX-homologous sequences to form PX-DNA is believed not to prevent fully homologous DNA duplexes from establishing this structure,[36,37] thereby suggesting a possible role of PX-DNA in the recognition of homology between DNA double helices.[24]

### 2.2. Paranemic Crossover DNA Cohesion

The most commonly used form of intermolecular cohesion between DNA double helices is by short (2−6 nt long) sticky ends that provide high intermolecular specificity.[38] However, the cohesive strength afforded by short sticky ends has been found insufficient for linking large objects together.[39] More



DOI: 10.1021/acs.chemrev.8b00207
*Chem. Rev.* XXXX, XXX, XXX−XXX

importantly, nonspecific hybridization may occur between undesired pairs of long sticky ends, which can compromise proper intermolecular recognition. An alternative form of intermolecular binding is available through the PX motif (called PX cohesion herein; see Figure 1c) where each of the two components contains a half-PX segment (a partially paired double-stranded structure) that is able to hybridize with another half-PX segment to form a full PX structure. PX cohesion has been used to connect topologically closed DNA molecules, which is not possible via sticky-ended cohesion.[40] Sequences of the unpaired regions of each half-PX segment, which are responsible for the fidelity of PX cohesion, can be programmed to provide intermolecular recognition with high specificity, similar to the short sticky ends. Furthermore, the length of the PX domains can be adjusted to provide the desired cohesive strength for linking large objects.[40]

## 3. PARANEMIC CROSSOVER DNA-BASED NANOMECHANICAL DEVICES

Nanoscale DNA machines and devices can be designed to change their conformational states in response to external stimuli, such as temperature,[41,42] pH,[43,44] and ionic conditions,[45,46] as well as to photoisomerization[47,48] and protein binding.[49,50] DNA devices can also be developed to undergo sequence-dependent conformational changes driven by toehold-mediated strand-displacement reactions (branch migration).[51] Compared to devices that act on environmental cues, sequence-dependent DNA nanomechanical devices allow for more precise addressability of particular device states by design.

### 3.1. PX–$JX_2$ Rotary Device

One type of such a sequence-dependent device is operated on the basis of interconversion between the PX structure (state) and its topoisomer, $JX_2$.[5] As shown in Figure 2, the early PX–$JX_2$ device consisted of a motor compartment in which one of the strands in the red and purple helices was interrupted and replaced with a pair of yellow set strands. These strands had unpaired single-stranded regions that acted as toeholds for initiating a strand displacement reaction. Removal and replacement of these set strands led to different states of the device. Specific pairs of set strands were used to fix the device in either the PX (yellow strands) or the $JX_2$ state (light blue strands). Starting from the PX state, addition of the full complements (fuel strands) to the yellow set strands displaced these strands from the PX state, leading to an unstructured frame. The energy used to drive such a device came from the extra base-pairings between the fuel and set strands. The fuel strands were biotinylated so that duplexes of the set strands and their complements could be removed by magnetic streptavidin particles. Addition of a pair of light blue set strands converted the frame to the $JX_2$ structure; addition of the light blue fuel strands again produced the frame; and addition of the yellow set strands restored the PX state. Each PX–$JX_2$ or $JX_2$–PX structural conversion resulted in a half-turn rotation between their helix ends as indicated by the letters in Figure 2. From this two-state PX–$JX_2$ rotary device, one could imagine that if $N$ different PX–$JX_2$ devices could be incorporated into a 2D or 3D DNA crystalline array, $2^N$ different structural states would be available for applications such as DNA-based universal computation.[13,14] This platform was further expanded to $3^N$ states by using a three-state device reported previously.[9] In addition to just relying on the toehold-mediated strand-displacement reaction to drive the device motion, switching between the two PX–$JX_2$ device states can also be driven by RNA strands via a cover-strand strategy.[8] The work suggests the potential of utilizing such a device in vivo, where endogenous RNA transcripts are largely single-stranded. Additionally, operation of two sets of PX–$JX_2$ devices have been achieved by using the same pair of set strands to perform reciprocal rotary motions synchronously.[11] These unique device setups have added new elements to the toolbox for use in nanorobotics and DNA computing.

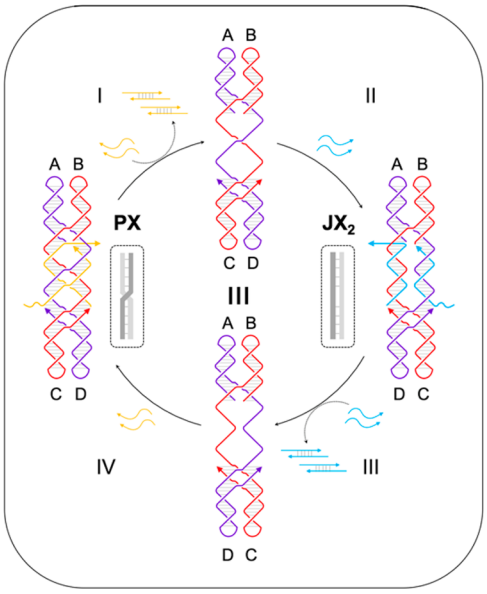


**Figure 2.** PX–$JX_2$ rotary device.[5] The PX state of the device is defined by the yellow set strands that can be removed by their complements (step I) to leave an unstructured frame. The addition of the light blue set strands (step II) converts the frame to the $JX_2$ structure, in which the top and bottom domains are rotated by a half-turn of DNA (about 180°) relative to their arrangement in the PX conformation (denoted by alphabetic labels). Steps III and IV reverse this process to return to the PX structure.

### 3.2. Polymer Assembly

The PX–$JX_2$ device has further served as a key component to assemble DNA nanomechanical machinery that enables the synthesis of products with desired sequences determined by the state of the PX–$JX_2$ device (Figure 3a).[6] In this system, two unique PX–$JX_2$ devices were used in succession to connect and control the relative orientations of a diamond-shaped motif and a pair of double-diamond-shaped wings. Programmed sticky ends on the outer edges of the diamond-shaped motifs (indicated by Arabic numbers in Figure 3a) were available to bind respective DX molecules that contained a continuous DNA strand extending from one end to the other. Changing the states of the two PX–$JX_2$ devices independently resulted in four ($2^2$) different combinations of sticky-end pairs flanking two PX–$JX_2$ devices. The pair of sticky ends between these diamond-shaped motifs could then bind one of six DX molecules in each of the two gaps. This process in turn directed the synthesis of four different product molecules upon ligation of the continuous strand in DX molecules. The state of the PX–$JX_2$ devices was solely established by the addition of DNA set strands, which had no transcriptional relationship with the final ligation product. Thus, this machinery carried the translation features of a ribosome. When arbitrary polymers


DOI: 10.1021/acs.chemrev.8b00207
Chem. Rev. XXXX, XXX, XXX–XXX

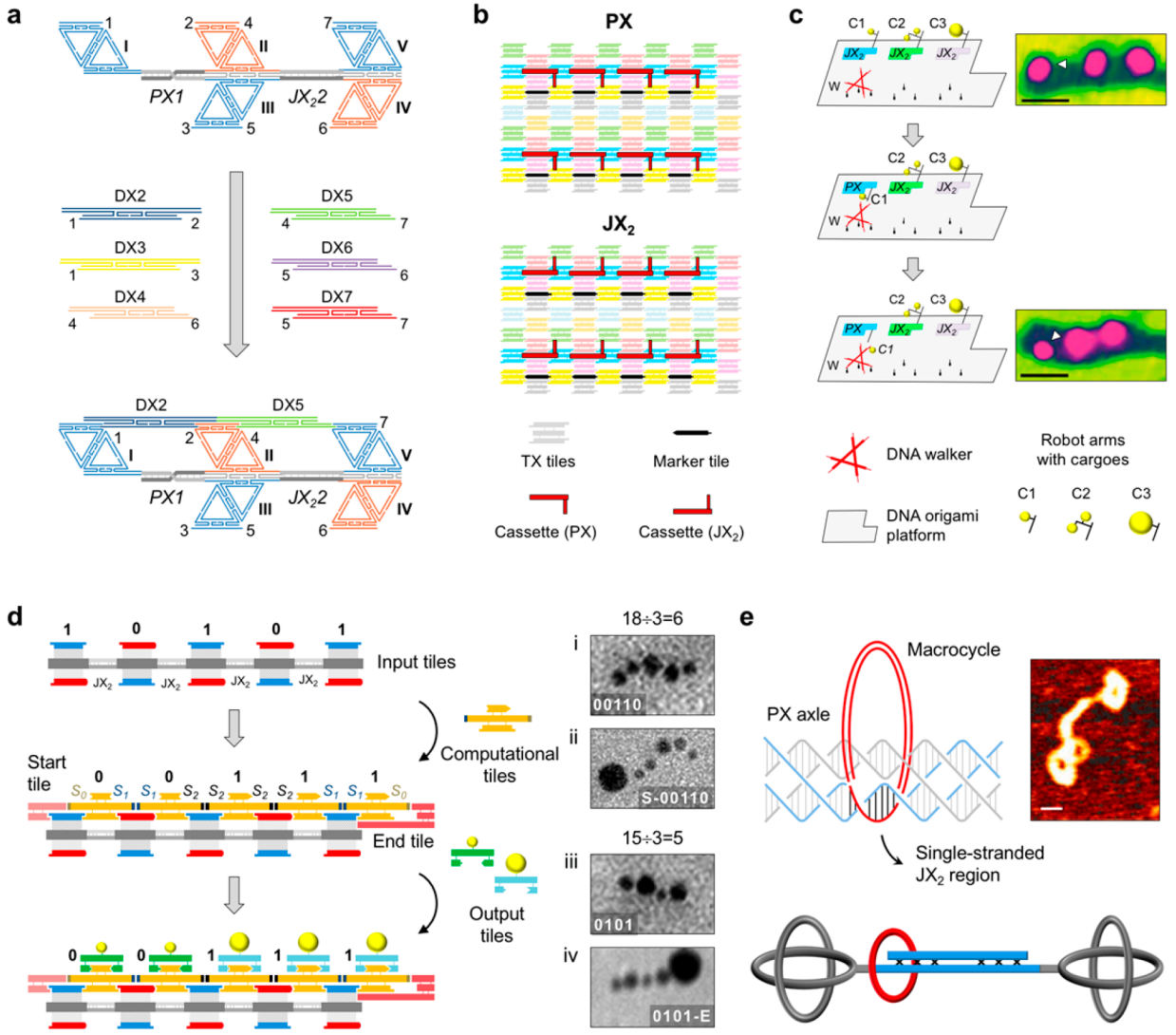


**Figure 3.** Paranemic crossover DNA-based nanomechanical devices. (a) Schematic of the translation device based on the PX–$JX_2$ system.[6] There is no transcriptional relationship between the set strands in the two PX–$JX_2$ devices and the sequences in the translated product. (b) Insertion of a device cassette into a DNA 2D array.[7] The eight TX tiles that form the array are shown in different colors. Cohesive ends are shown to be the same geometrical shape, although they all contain different sequences. (c) Nanoscale assembly line on a DNA origami platform.[12] Three different PX–$JX_2$ devices hold cargoes C1 (5 nm particle), C2 (a pair of 5 nm particles), and C3 (10 nm particle). Switching of the device from $JX_2$ to PX state positions the cargo toward the DNA walker (W) for pickup. The illustration shows only the pickup of the first cargo. Scale bars: 50 nm. Adapted with permission from ref 12. Copyright 2010 Macmillan Publishers Ltd. (d) DNA transducer based on a sequence of input tiles connected by PX–$JX_2$ devices.[13] Assembly of a set of computational tiles and output tiles provides a specific output based on the input provided. TEM results of the computation (division of numbers 18 and 15 by 3 in binary) are shown on the right (i, iii). Zeroes and ones are represented by 5 and 10 nm gold nanoparticles, respectively. Start or end tiles can be tagged with 15 nm streptavidin-gold nanoparticles (ii, iv) to provide a reference of where the gold nanoparticle string starts or ends. Reprinted with permission from ref 13. Copyright 2012 The Royal Society of Chemistry. (e) DNA rotaxane with a PX axle.[55] The macrocycle is attached by a complementary single-stranded region on the $JX_2$ portion of the axle. AFM image reprinted with permission from ref 55. Copyright 2012 Wiley–VCH.

were attached with the DX molecules, this ribosome-like system could template the formation of diverse and unprecedented polymers with highly controlled lengths and compositions.

### 3.3. DNA Robot Arm

A PX–$JX_2$ device has been placed and operated on a DNA 2D array through a cassette that was designed to consist of a PX–$JX_2$ device to drive the motion, an insertion domain to attach to the 2D array base, and a hairpin robot arm to report the device state.[7] The 2D array platform was formed from TX molecules whose middle domains contained sticky ends complementary to those in the insertion domain of the cassette or a DNA duplex that acted as a reference marker for determining the robot arm position and therefore the device state (Figure 3b). Specifically, operation of the device was reported by the directionality of the robot arm: it pointed toward the marker in the PX state or away from the marker in the $JX_2$ state. This study provides an example of controllable mechanical motion via a sequence-triggered nanorobotic system within a fixed frame of reference. Furthermore, the strategy of using a PX–$JX_2$-containing cassette and hairpin robot arm has been adapted for operating a nanoscale assembly line on a 2D DNA origami platform (see section 3.4).


DOI: 10.1021/acs.chemrev.8b00207
Chem. Rev. XXXX, XXX, XXX–XXX

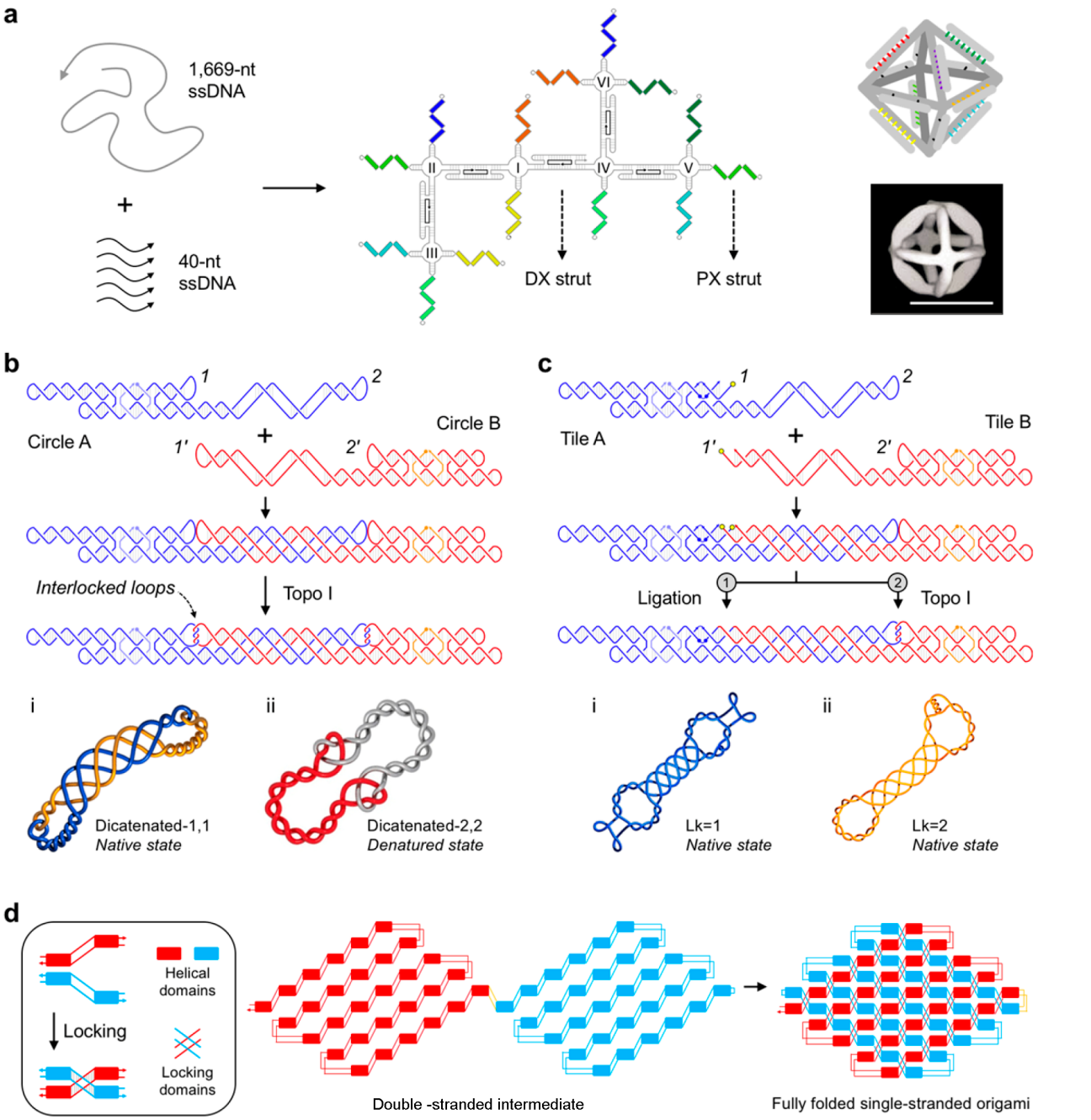


**Figure 4.** Paranemic crossover DNA-based nanoscale objects. (a) Folding of a 1.7 kb single strand and five short complementary strands, resulting in an octahedron with five DX and seven PX struts.[15] PX cohesive segments shown in the same color indicate PX complementarity. Note that within each of these segments the strand is partially complementary to itself and partly complementary to its complementary half-PX indicated by the same color. Adapted with permission from ref 15. Copyright 2004 Macmillan Publishers Ltd. (b) PX cohesion of two circles A and B, followed by topo I treatment that interlocks the cohesive loops.[19] Complementary loops are denoted by 1−1′ and 2−2′. Linking of one or both cohesive loops results in a mono- or dicatenated complex. (i, ii) Knotilus[70,71] representations of the native state of a dicatenated complex ($Lk$ = 1 for both links) and denatured state of a dicatenated complex ($Lk$ = 2 for both links), respectively. (c) DNA tiles A and B that can cohere via PX-cohesive tails and contain both complementary sticky ends (1−1′) and cohesive loops (2−2′).[19] Annealed complexes can be knotted by ligation of sticky ends followed by topo I treatment that interlocks the cohesive loops. 5′-Phosphates required for the ligation process are denoted by yellow circles. (i, ii) Knotilus[70,71] representations of two knots in their native states with (i) $Lk$ = 1 and (ii) $Lk$ = 2. All scale bars are 20 nm. Knotilus images reprinted from ref 19. Copyright 2015 American Chemical Society. (d) Left: Schematic depicting the formation of a locking domain based on PX cohesion. Right: Illustration showing the double-stranded intermediate and fully formed single-stranded origami structure.[66]

### 3.4. Nanoscale Assembly Line

The concept[7] of DNA cassettes that contain a PX−JX$_2$ device and a robot arm has been successfully adapted for constructing a proximity-based nanoscale assembly line[12] on a 2D DNA origami platform.[52] As illustrated in Figure 3c, the assembly line consists of three important components: a rectangular-shaped DNA origami[52] that acts as the assembly line platform, cassettes containing three independent PX−JX$_2$ devices and robot arms that serve as programmable cargo-donating devices, and a DNA walker that can move on the track from device to


DOI: 10.1021/acs.chemrev.8b00207
Chem. Rev. XXXX, XXX, XXX−XXX

device to pick up cargoes. Each robot arm of the three PX−$JX_2$ devices attached in succession on the origami platform contains a different cargo: a 5 nm gold nanoperticle (AuNP) on C1, a pair of 5 nm AuNPs on C2, and a 10 nm AuNP on C3. Design of the walker is based on a tensegrity triangle[53] with three hands and four feet, all consisting of single-stranded DNA regions. The feet of the walker can bind to specific single-stranded extensions protruding from the origami platform and facilitate locomotion. When a device is switched from an off-state ($JX_2$) to an on-state (PX), the robot arm of the device will position the corresponding cargo (AuNP) toward the DNA walker (W) for pickup. As the walker traverses the track, the hands can pick up one of the eight ($2^3$) possible combinations of cargoes made available and controlled by the state of the three independent PX−$JX_2$ devices. In addition to the switching between PX (on) and $JX_2$ (off) states, the walker movement and the cargo transfer from robot arms to walker hands are also driven by toehold-based strand displacement.[51] Similar to the ribosome-like machinery,[6] the set strands used to control the states of three individual PX−$JX_2$ devices herein have no transcriptional relationship with the final DNA−AuNP products. Furthermore, the synergy among these independent PX−$JX_2$ devices has provided programmability and spatial control of an assembly line, which can be further employed in the assembly of other external entities.

### 3.5. DNA Transducer

By adapting the strategy used in the assembly of ribosome-like machinery (discussed in section 3.4), a series of PX−$JX_2$ nanomechanical devices have been aligned sequentially to form a 1D transducer that divides a number by 3.[13] In this transducer (Figure 3d), the computational input consisted of individual two-state PX−$JX_2$ devices that controlled the orientations of six-domain-flat (6DF) DNA motifs; a set of TX motifs serve as the computational or end tiles, and the output was denoted by chelator DX tiles containing different-sized AuNPs. More specifically, the transducer's input layer was formed by a linear arrangement of five 6DF motifs connected by four PX−$JX_2$ devices. The 6DF motifs contained two different sticky ends on the top or bottom domain to define each binary bit, 1 or 0, of the computational output, which was controlled by the configuration of each of the PX−$JX_2$ devices as the input. As the device changed its state, the top or bottom sticky ends of the 6DF motif bound to complementary sticky ends on the lower domain of a corresponding computational TX tile (indicating 0 or 1) that in turn would determine which chelator DX tile fits on top of the TX tile to display the computation output. The chelator tile for binary bit 0 carried a 5 nm AuNP and bound to a 0-indexing TX, while the chelator tile for binary bit 1 carried a 10 nm AuNP and bound to a 1-indexing TX. The output was thus displayed by a series of 5 and 10 nm AuNPs with different orders [Figure 3d(i,iii)]. In addition, start (DX) or end (TX) tiles tagged with 15 nm AuNP were used to distinguish the start or end of the output nanoparticle strings under TEM imaging [Figure 3d(ii,iv)]. This transducer was used to successfully demonstrate the division of a number by 3 (in binary). In addition, a similar DNA transducer that involves reciprocal PX−$JX_2$ devices[11] has been constructed for programmable molecular choreography, with DX triangles as topological markers, to display the computation output.[54] Furthermore, successful integration and operation of PX−$JX_2$ devices in 1D space[6,13] has paved the way for expanding the platform of operating such nanomechanical devices in 2D space.

### 3.6. DNA Rotaxanes

Apart from being used as a motor for a device, PX and $JX_2$ structures have also been used to assemble the axle of a DNA rotaxane to reinforce its stiffness (Figure 3e)[55] to ensure that the molecular rotaxane assembly can better carry out directional mechanical motion compared with an early version of the rotaxane-based mechanical device built on a double-stranded DNA axle.[56] In the new design, the $JX_2$ portion of the rotaxane axle contains a single-stranded gap that can hybridize with a complementary single-stranded region of the otherwise double-stranded macrocycle (indicated in red in Figure 3e). The ends of the rotaxane are ligated to spherical DNA stoppers to prevent the macrocycle from getting off the axle. Addition of the so-called release oligonucleotides, complementary to the single-stranded region of the macrocycle, releases the macrocycle from the $JX_2$ attachment point, thus resulting in a stable DNA rotaxane with an interlocked, fully mobile macrocycle. Such rigid rotaxane architectures can be integrated into higher-order assemblies to enable the study of biological phenomena that involve molecular motors.

## 4. PARANEMIC CROSSOVER DNA COHESION-MEDIATED ASSEMBLY OF DNA OBJECTS

### 4.1. Construction of DNA Polyhedra

Construction of DNA objects with a finite size depends on programmed sticky ends as a main approach for intra/interobject cohesion. Some such examples are cubes,[57,58] tetrahedra,[59] octahedra,[60,61] and icosahedra.[38] Paranemic cohesion offers an alternative strategy for intramolecular interaction when making DNA objects. One such DNA object is a DNA octahedron constructed by folding a 1.7-kilobase-long single-stranded DNA by use of PX cohesion for intramolecular connection (Figure 4a).[15] Specifically, initial folding of the long single strand is assisted by five short [40 nucleotides (nt) each] synthetic DNA strands, which form an intermediate flat structure composed of five DX struts, and 14 half-PX struts, each of which exhibits PX complementarity to one other strut (coded with the same color in Figure 4a). The five DX motifs formed after the initial folding serve as five of the 12 edges of the octahedron; the 14 PX-cohesive segments combine intramolecularly to form the remaining seven edges upon final folding of the octahedron. The PX motif used in making this DNA octahedron contains major- and minor-groove separation of six and four base pairs (PX-6:4), which was constructed and characterized before but was suggested to be unstable in a four-strand complex.[4] The observation is that four-strand PX molecules seem most sensitive to the major/minor groove ratio. As noted above, the 6:4 PX molecule is stable when there is a large structure, of which the PX (6:4) struts are a part, that may help to stabilize the strands more readily than four free strands. In plasmids, where the whole interaction is intramolecular, 11:5 PX molecules have formed under superhelical stress.[24,62] In addition to tile-based DNA objects assembly, we want to point out that the DNA origami strategy[52] is another route to create larger DNA objects,[63−65] however, without use of sticky-ended or PX cohesion strategy for intramolecular linkages.


DOI: 10.1021/acs.chemrev.8b00207
Chem. Rev. XXXX, XXX, XXX−XXX

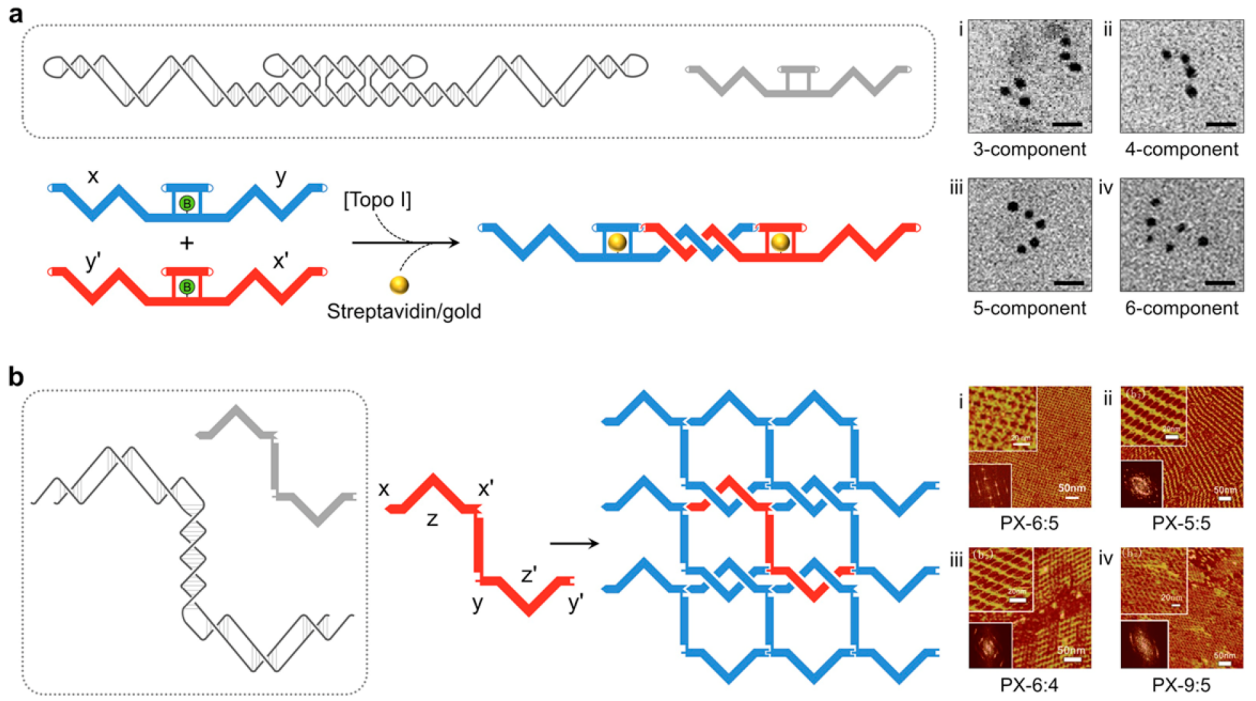


**Figure 5.** Assembly of 1D and 2D arrays by paranemic crossover DNA cohesion. (a) 1D array formed by PX cohesion of DNA tiles.[18] The loops at the ends of the DNA tile can be mechanically interlocked via topo I treatment. Addition of biotin moieties (shown as green circles) on component tiles provides an attachment site for streptavidin/gold conjugates. This strategy can be used to create infinite 1D arrays as well as finite arrays from specific numbers of component DNA tiles. TEM images of (i) three-, (ii) four-, (iii) five-, and (iv) six-component arrays are shown on the right. Scale bars: 50 nm. TEM images reprinted from ref 18. Copyright 2015 American Chemical Society. (b) DNA 2D arrays formed by a Z-shaped motif that coheres via T-junction formation in the horizontal direction ($x/x'$ and $y/y'$) and via PX cohesion in the vertical direction ($z/z'$).[20,21] Complementary regions are denoted as shape-fitting geometrical shapes. 2D arrays resulting from variations of the PX motifs are shown on the right: (i) PX-6:5, (ii) PX-5:5, (iii) PX-6:4, and (iv) PX-9:5. Reprinted with permission from refs 20 and 21. Copyright 2016 and 2017 The Royal Society of Chemistry.

### 4.2. DNA Catenanes and Knots

Apart from providing intramolecular connection, PX cohesion has also been used to cohere two topologically closed DNA motifs containing a pair of sequence-complementary loops to produce various catenated and knotted structures.[18] As shown in Figure 4b, each circle consisted of a DX domain, a half-PX tail, and two intermolecular-kissing loops. The two circles could cohere via DNA base pairing between two half-PX segments and between each of the two opposing loops (labeled 1 or 1′ and 2 or 2′ in Figure 4b) containing complementary sequences. The hydrogen-bonding-based noncovalent interaction between the two circles could be converted into a topological bond by topo I treatment, which enables strand passage of the cohesive loops. The resulting complex could be singly or doubly linked depending on whether one or both loops were catenated. In addition, each of the catenated loops could be linked either once or twice due to the flexibility of the 16-base-pair complementary tract in the loops, leading to the formation of multiple mono- and dicatenated products [one example for each is shown in Figure 4b(i,ii)]. For the creation of knotted structures, the component PX tiles containing one set of sticky ends and one intermolecular-interacting loop have been designed and used. As shown in Figure 4c, the sticky end on the DX domain of tile A contains 3′−3′/5′−5′ linkages, while tile B contains a regular sticky end on the tip of the half-PX tail. The two tiles can thus cohere via Watson−Crick complementarity between the two half-PX segments (PX cohesion), the complementary loops, and the sticky ends. Topo I treatment on the cohesive loops resulted in the formation of knots with a linking number of 1 or 2 depending on the length (11 or 16 nt) of the complementary tract carried in the loops [Figure 4c(i,ii)]. Circular constructs connected by paranemic cohesion and then interlinked by topo I can be used to construct novel DNA objects and arrays that can therefore withstand heat and chemical denaturation and better resist digestion by DNA exonuclease.

### 4.3. Single-Stranded Origami

Recently, a strategy was developed to create origami structures from only a long single-stranded DNA and RNA.[66] Distinct from the conventional origami assembly method that relies on hundreds of staple strands for assembly and sticky-ended cohesion for intermolecular linkage, this so-named single-stranded origami (ssOrigami) strategy employs partially complementary double-stranded regions and takes advantage of the unique PX cohesion capability to connect topologically closed units in a sequence programmable manner. More specifically, as illustrated in Figure 4d, the long single strand has self-complementary regions resulting in a double-stranded intermediate. The unpaired locking domains fold in a half-PX fashion, resulting in a fully assembled origami structure via PX cohesion. The ssOrigami strategy is able to create DNA structures as large as a 10 682-nt rhombus shape and RNA structures containing up to 6337 nt, demonstrating a manifold improvement in the complexity of structures self-folded from ssDNA or ssRNA.[22,67−69] The feasibility of this strategy to create RNA nanostructures points toward the use of PX cohesion not just in a DNA context but also in RNA-based designs. Moreover, a key feature of ssOrigami is that the


DOI: 10.1021/acs.chemrev.8b00207
Chem. Rev. XXXX, XXX, XXX−XXX

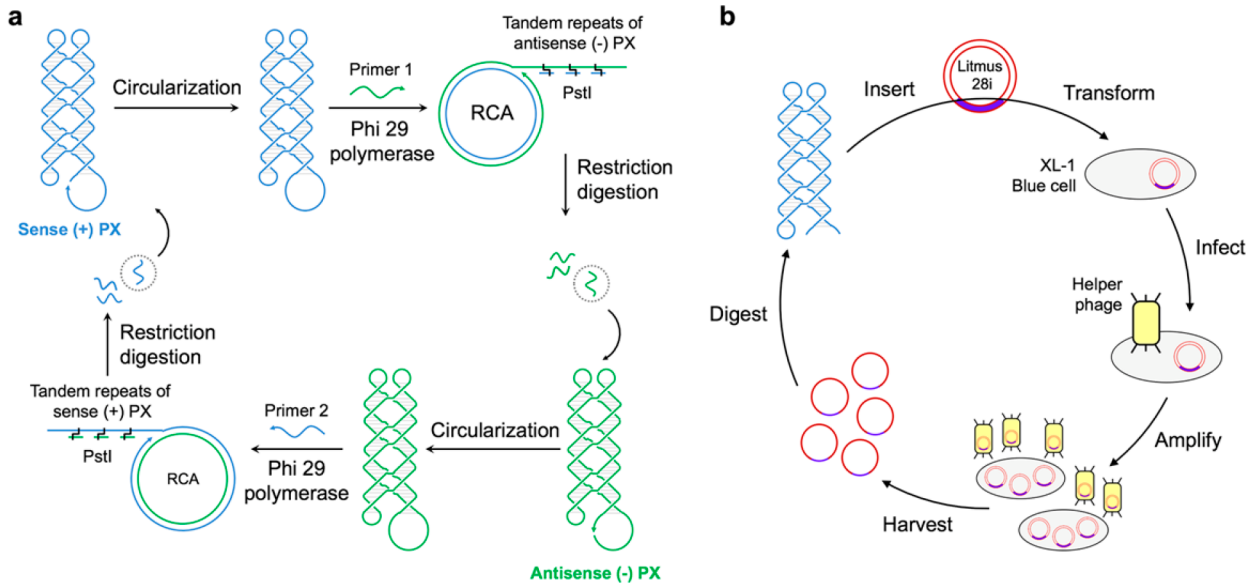


**Figure 6.** Replication and biological relevance of paranemic crossover DNA. (a) Schematic of rolling-circle amplification (RCA)-based enzymatic replication of PX-DNA.[22] (b) Schematic drawing showing in vivo replication of PX-DNA.[23] The single-stranded DNA that can fold into a PX structure is inserted into single-stranded M13mp18 viral DNA, transformed into XL1-Blue cells, and amplified in bacteria in the presence of helper phages. High copy numbers of cloned nanostructures are obtained by standard molecular biology techniques.

structure can be replicated by use of both in vitro[15,22,67,68] and in vivo protein machineries.[23,67]

## 5. PARANEMIC CROSSOVER DNA-MEDIATED FORMATION OF DNA ARRAYS

### 5.1. One-Dimensional Arrays via Paranemic Crossover DNA Cohesion

The strategy of connecting topologically closed units by PX cohesion and a pair of kissing loops has also been used in the creation of catenated 1D arrays[18] composed of two component circular tiles containing a central DX domain flanked on both sides by PX cohesive tails (half-PXs). As shown in Figure 5a, the top part of the DX domain and either end of the PX tail is closed by a 26 nt stem−loop. The two circular tiles cohere in an alternating fashion to form a 1D array via PX cohesion and loop kissing. The arrayed tiles can further be topologically linked after topo I treatment to produce a polycatenated linear array with the repeated units still staying connected even at high temperatures when all the DNA base pairs are denatured. Such tiles, when modified to contain biotin moieties, have acted as scaffolds to spatially position streptavidin-coated gold nanoparticles into 1D arrays. Sequence of these PX cohesive tiles can be programmed to create *n*-component finite arrays and display specific numbers of gold nanoparticles [Figure 5a(i−iv)].

### 5.2. Two-Dimensional Arrays via Paranemic Crossover DNA Cohesion

Similar to the self-assembly of DNA objects, formation of DNA 2D arrays from rigid DNA motifs is mainly achieved via sticky-ended cohesion.[31,32] Earlier attempts at using PX cohesion as an alternate strategy to create DNA 2D arrays were not successful. For example, DX triangle motifs with PX cohesive segments extended from each edge were designed to form a trigonal pseudohexagonal 2D array but resulted only in ill-formed arrays that contain cavities flanked by four or six triangles.[16] DX triangle motif with double PX cohesion was also unsuccessful in forming the designed arrays,[16] although the same motif was able to successfully produce trigonal pseudohexagonal arrays when assembled with sticky ends.[72] Although the PX motif is believed to be rigid, its helical structure is still not as well-characterized as the B-DNA structure in sticky ends.[73] The early attempts just assumed a B-DNA helical structure of PX motif, which seemed to be inaccurate. This has been evidenced by the formation of unexpected bent intermolecular structures of PX in the attempts at making trigonal pseudohexagonal 2D arrays,[16] which suggests that the periodicity of PX cohering segments deviates from that of canonical B-DNA.

To this end, a Z-shaped DNA motif (called Z-tile herein) that involves both PX and sticky-ended cohesions has recently been designed and successfully applied to form single-tile-based DNA 2D arrays.[20] Shown in Figure 5b, the Z-tile is a two-stranded complex that contains a central vertical double-helical domain with two half-PX regions ($z/z'$ in Figure 5b) extending above and below the DNA duplex, in opposite directions. Each half-PX is flanked by a sticky end on one side and a single-stranded loop on the other that can pair with their complementary regions on the other half-PX region ($x/x'$ or $y/y'$ in Figure 5b). Upon annealing, Z-tiles will associate via PX cohesion in the vertical orientation and via sticky-end-mediated T-junction formation in the horizontal orientation that leads to the formation of periodic 2D arrays. Compared to other PX variations (PX-5:5, PX-7:5, PX-8:5, PX-6:4, and PX-7:4) tested in the study, the Z-tile with a PX-6:5 structure was found to yield a larger and more uniform 2D lattice [Figure 5b(i)]. This is possibly due to the stress associated within PX-5:5, PX-7:5, PX-8:5, PX-6:4, or PX-7:4 motifs that deviate from canonical B-form DNA much more than a PX-6:5 motif. An immediate follow-up study[21] has tested this hypothesis by showing that such stress can be relieved by the addition or deletion of base pairs in the PX region of the Z-tile for tuning the major- and minor-groove separations of the PX variants closer to that of B-DNA, thereby yielding larger and more uniform 2D lattices [Figure 5b(ii−iv)].


DOI: 10.1021/acs.chemrev.8b00207
*Chem. Rev.* XXXX, XXX, XXX−XXX

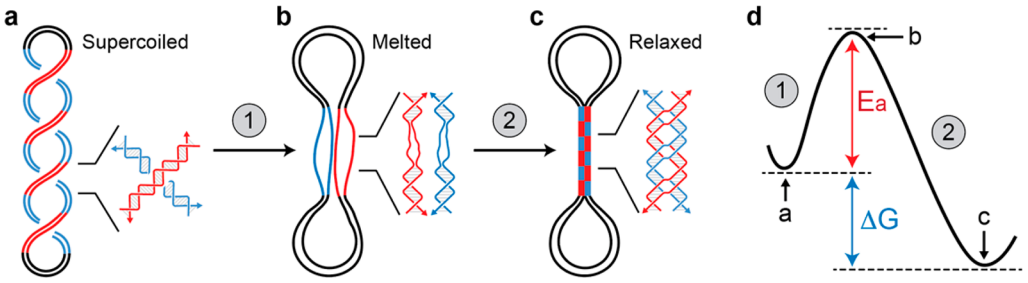


**Figure 7.** Schematics of fusing two homologous duplexes into a shaftlike structure, activated by the free energy associated with supercoiled plasmid. (a) Interwound structure that has not contorted itself to relax; red parts of the backbone are closer to the reader than blue parts. B-DNA is drawn to the right in color coding that corresponds to the molecule on the left. (b) Transition state in plasmids from B-DNA (supercoiled) to PX-DNA (relaxed). DNA base pairs in homologous duplexes are melted by use of the free energy associated with supercoiled plasmid. (c) Molecule that has relaxed by forming a PX structure, drawn as alternating red and blue boxes on the left, with the molecular structure on the right.[24] PX-induced relaxation will lead to a dumbbell structure, with a long shaft flanked by loops on either end. The position of the inserted homologous DNA will affect the position of the shaft and the sizes of the loops. (d) Energy levels associated with the transition from supercoiled to intermediate (1) to relaxed plasmids (2). $E_a$, activation energy; $\Delta G$, gained free energy.

## 6. PARANEMIC CROSSOVER DNA AMPLIFICATION USING BIOLOGICAL MACHINERIES

DNA oligonucleotides used for the self-assembly of DNA motifs (including PX) and DNA arrays are mainly obtained from phosphoramidite chemistry-based[74] automated synthesis on a solid support. However, this commonly used DNA synthesis approach is still expensive, and more importantly, it is an unaffordable and inefficient approach to producing a long single-stranded DNA that itself can fold into a nanostructure. Hence, a more economic and efficient method of producing such long single-stranded DNA is desired. It has been reported that circular single-stranded DNA molecules with the propensity to fold into a PX structure can be amplified both in vitro, via rolling-circle amplification (RCA) (Figure 6a),[22] and in vivo, via cell cloning (Figure 6b),[23] with high efficiency and sequence fidelity. Impact of these studies is 2-fold. First, results from these experiments suggest that PX structure can survive complex enzymatic processes even in vivo, which is supported by the fact that both replications proceed at 37 °C, a temperature lower than the PX melting temperature,[4] when PX structure should still be largely intact. Thus, RCA-involved or in vivo cloning-involved enzymatic machinery is able to efficiently unwind, at least locally, then pass through and finally copy the whole PX molecule. Second, these studies also provide economical, reliable, and high-yield strategies for large-scale production of long single-stranded DNA molecules, capable of folding into DNA objects by themselves[67] or into 2D arrays together with other DNA oligonucleotides.[75,76]

Asymmetric polymerase chain reaction (PCR)[77] was also suggested as a viable strategy, mainly to create long ssDNAs that serve as DNA scaffolds for DNA origami assembly. Along this direction, recent advances in asymmetric PCR provide control over ssDNA sequence completely from 3′ to 5′ end; these advances were used to produce ssDNA of lengths ranging from 100 nt up to 15 000 nt, and the process can be purely enzymatic.[65,78] Such developments could be valuable for novel DNA constructions and specifically for PX cohesion-assisted ssOrigami assembly (discussed in section 4.3).[66]

## 7. PARANEMIC CROSSOVER DNA AND DNA HOMOLOGY RECOGNITION

It has been reported that pairing of chromosomal regions with similar or identical DNA sequences occurs in the absence of DNA breakage and homologous recombination (HR). This so-called recombination-independent homologous pairing (abbreviated to RIHP herein) exists in a variety of cellular contexts[79] and is known to play vital roles in many important biological processes.[80−82] Previous studies have uncovered the presence of higher-order DNA structures when two homologous DNA duplexes associate under physiological conditions in vitro, yet they have not provided much insight into the underlying molecular mechanism.[83,84] McGavin[36] and Wilson[37] have proposed paranemic motifs that are appealing models of homologous recognition, helpful to elucidate some homologous pairing data.[85] However, formation of such motifs has not been demonstrated experimentally. PX has recently been implicated as the DNA motif in RIHP,[24] supported by experimental data that demonstrate the fusion of two DNA duplexes into a higher-order structure with predicted length and position when duplexes carrying a PX-homologous sequence[4] are cloned in a negatively supercoiled plasmid. As illustrated in Figure 7, this fusion is believed to be activated by Gibbs free energy[86] (associated with supercoiled DNA[87] in prokaryotes, as circular plasmids, and in eukaryotes, as packed around histones in chromatin) and driven by the relaxation of supercoiling via forming PX structure (the formation of PX-DNA can untwist B-DNA) in the presence of DNA homology. The observation agrees with the note that every functional output of DNA is shaped by mechanical properties conferred by DNA topology and supercoiling.[88] Moreover, atomic force microscopic (AFM) imaging of the patterns generated in vitro and in vivo after psoralen cross-linking further proves that strands in the two homologous regions form DNA crossovers, like those formed in PX, rather than a bare DNA−DNA backbone juxtaposition.[24] Departing from this point, more in vivo effort is needed to elucidate the biological functions of PX motif in RIHP.

## 8. CONCLUSION AND FUTURE DIRECTIONS

The PX motif carries distinct features in at least three different aspects: as a structural and intermolecular connecting motif in the self-assembly of DNA nanostructures (section 8.1), as a motor component of functional nanomechanical devices (section 8.2), and as a potential structural motif in DNA homology recognition (section 8.3).



DOI: 10.1021/acs.chemrev.8b00207
Chem. Rev. XXXX, XXX, XXX−XXX

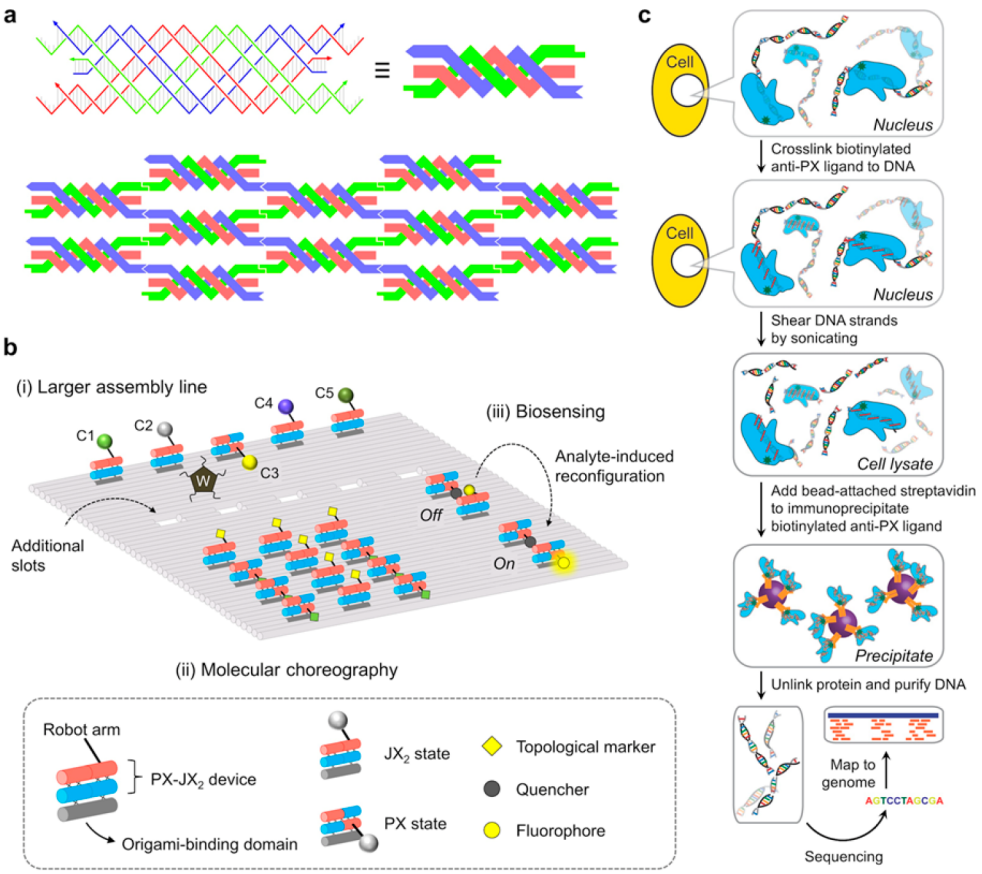


**Figure 8.** A few proposed ideas involving paranemic crossover DNA. (a) Structural diagram of a three-helical paranemic crossover (TPX) motif with three double helices interwoven in a paranemic fashion (top).[91] Such motifs tailed with sticky ends and optimized periodicity could self-assemble into a 2D array (bottom). The three interweaving double helices are shown in different colors for clarity, while complementary sticky ends are shown as complementary geometrical shapes. (b) Applications of PX–$JX_2$ nanomechanical device. (i) Scaled-up assembly lines on larger DNA origami: five different cargoes (C1–C5) are denoted as colored spheres, and the third cassette is in the PX state, thus positioning cargo C3 toward the walker (W). Additional slots on the origami platform for insertion of PX–$JX_2$ devices are also shown. (ii) Molecular choreography: A series of PX–$JX_2$ devices carrying topological markers can be designed to indicate features depending on the states of the devices. Topological markers (diamond shapes) in PX and $JX_2$ states are shown in different colors for clarity (yellow for $JX_2$ and light green for PX). In the example shown, the $JX_2$ states of the devices show a topological feature (yellow diamonds) in a T-shape. (iii) Biosensing based on analyte-induced reconfiguration: Two PX–$JX_2$ devices, one with a quencher (gray circle) and one with a fluorophore (yellow circle), can be positioned so that the fluorescence is quenched in the off-state. Addition of a target molecule can be designed to reconfigure one of the devices, thus moving the fluorophore away from the quencher, resulting in a fluorescent signal (on-state). (c) Workflow diagram illustrating the principles of genome-wide chromatin immunoprecipitation sequencing (ChIP-Seq), where the location of DNA binding sites on the genome for anti-PX ligand could be investigated. In short, biotinylated anti-PX ligand introduced in living cells is cross-linked by formaldehyde to the DNA to which it is bound. Following cross-linking, the cells are lysed and the DNA is broken into small pieces (0.2–1.0 kb) by sonication. The ligand–DNA complex can be immunoprecipitated out of cellular lysates by use of streptavidin-coated beads (e.g., magnetic or agarose beads). The ligand–DNA complexes are then purified and heated to reverse the formaldehyde cross-linking, resulting in the separation of DNA from the ligands. The isolated DNA fragments can be sequenced by Illumina sequencing, a next-generation sequencing technology. Massively parallel sequence analyses can then be carried out in comparison with existing whole-genome sequence databases to determine temporal and spatial parameters of homologous interactions at single-nucleotide resolution.

### 8.1. Paranemic Crossover DNA in Structural DNA Nanotechnology

In the structural aspect, the paranemic nature of the PX motif is useful for the construction of topologically closed DNA structures, which will provide enhanced stability to complex structures against enzymatic degradation (specifically by DNA exonucleases). As an alternative to sticky-ended cohesion, PX cohesion is able to afford cohesive strength for linking large objects while keeping a high intermolecular interacting specificity, as sticky ends do. In this context, the mechanical rigidity of PX molecules has been studied by MD simulations. Studies revealed that the stretch modulus of PX and its topoisomer $JX_2$ structure is significantly higher (~30%) compared to normal B-DNA of the same sequence and length.[89] Molecular dynamics simulations have also provided atomic models of both PX and $JX_2$ structures.[35,90] Despite these simulated structures of PX and the recent success using PX in the formation of 2D arrays,[20,21] characteristics of PX-DNA at the atomic level from experimental data are still missing. Obtaining crystal structure of PX will help to improve the design of PX and its derivatives (e.g., three-helical paranemic crossover,[91] or TPX)-involved nanostructures (e.g., TPX 2D array shown in Figure 8a) and nanodevices. Furthermore, knowing the molecular structure of PX-DNA will assist in designing and evolving an anti-PX ligand to explore the implicated biological functions of the PX motif better in


DOI: 10.1021/acs.chemrev.8b00207
Chem. Rev. XXXX, XXX, XXX–XXX

RIHP (discussed in section 8.3). One possible solution is to make a new PX-carrying motif derived from the recently reported Z-tile[20] design to form a 3D DNA crystal for directly resolving the PX atomic structure via X-ray diffraction. Incorporating a PX component in a tensegrity triangle motif for rationally designed 3D DNA crystals is also a potential route to this end.[92] Another route is to assemble individual PX molecules onto a large 2D DNA framework such as DNA brick crystals[93] with a precise spatial arrangement or to use DNA origami-based molecular supports[94] and then to image the whole assembly for achieving PX atomic structure by X-ray free electron laser (XFEL) holography[95] or cryo-electron microscopy (cryo-EM).[96]

The PX molecules discussed in this review are assembled by traditional Watson−Crick base pairing. It would be worth investigating formation of the PX complex by using component strands that may contain modified nucleotides,[97] nontraditional base pairs[98] or xeno-nucleic acids.[99] DNA modifications are known to occur in nature,[100] and understanding the thermodynamics, structural characteristics, and resulting stability of PX complexes involving modified nucleotides could shed light on any biological relevance such as enzymatic activity on these complexes. Moreover, incorporation of unnatural base pairs is known to enhance the stability of DNA nanostructures.[101] Thus, PX motifs containing such alternate bases and base-pairing patterns might provide additional capabilities for structural DNA nanotechnology in the creation of robust architectures.

### 8.2. Paranemic Crossover DNA in Nanomachines

As the motor component of nanomechanical machines and devices, it is plausible to use the PX−$JX_2$ device on a structural scaffold to position reactants spatially and to direct proximity-enhanced chemical reactions as done previously, based on a simple DNA duplex−triplex transition.[102] The assembly line constructed with the PX−$JX_2$ device was programmed to have a DNA walker pick up any combination of cargoes from three different stations.[12] The number of stations is limited mainly by the size of the assembly line platform. Larger 2D DNA origami platforms[103] are now available and could be used to increase the number of stations on an assembly line from which the walker can pick up cargoes [Figure 8b(i)]. The device could also be programmed to reload after the first round of cargo pickup and delivery. Moreover, similar to previous reports that use topological markers for AFM,[104] PX−$JX_2$ device can be used to direct molecular choreography and create specific patterns based on molecular cues [Figure 8b(ii)]. PX−$JX_2$ devices integrated on a 2D DNA origami platform can sense the addition or presence of a target analyte that induces a conformational change between PX and $JX_2$ states through the release of specific fuel or set strands (e.g., ref 105). Fluorescent signals can be used as the readout for such a nanoscale-sensing array, as illustrated in Figure 8b(iii). Previous reports have shown RNA versions of paranemic motifs to be useful in biosensing.[106,107] This indicates that similar strategies could be employed that use the DNA version of PX for applications in biology and medicine. In principle, any application requiring two states in different spatial orientation can be achieved by use of a PX−$JX_2$ device.

### 8.3. Paranemic Crossover DNA in Biology

On the biology front, existing evidence has suggested that PX-DNA may be formed during homologous pairing (HP), but results are still inconclusive. Further investigation of PX biological functions is needed to obtain more in vivo evidence, by either applying conventional biological methods or developing new molecular and genetic tools. One possible idea for such investigation that uses established methods is to examine the effect of unusual PX structure on the regulation of transcription initiation and elongation, as previously studied with i-motifs.[108] Since pairing of homologous DNA is a conservative biological process, it is hard to raise an antibody against HP/PX-DNA based on an immune response in the animal. In this context, RNA aptamers or protein-based molecular ligands with high PX affinity and specificity can be sorted by directed-evolution approaches.[109−111] Acquisition of such an anti-PX/HP ligand may open up new avenues of research for a better understanding of homologous search/pairing-involved biological processes. These studies can be carried out by combining anti-PX ligand-based immunoprecipitation[112] with other advanced biotechnologies such as next-generation Illumina sequencing[113] and LC−MS (liquid chromatography−mass spectrometry) proteomics.[114,115] These combinatory approaches will provide comprehensive information on HP and its related biological activities (e.g., change of nuclear architecture, synapsis, meiosis, and HR) at a genomewide scale but with single-nucleotide or single-molecule resolution. For example, a deep-sequencing-based genomewide HP profiling strategy (Figure 8c) will likely enable the extraction of temporal and spatial parameters of homologous interactions and assist in understanding how HP constrains HR, in a wide variety of organisms and cell types or in a single cell type but at different developmental stages. Visual HP profiling may also provide insight into diverse genetic mysteries such as chromosome segregation/stability, correlation between nuclear architecture/organization and DNA repair, molecular mechanisms of genome manipulation, and spatial arrangement of transcriptional units. All of these will aid our understanding of the coordination of gene expression. LC−MS-based proteomics can survey protein binding partners that coimmunoprecipitated with anti-PX ligand, which in turn will facilitate the study of protein−HP complexes. Additionally, super-resolution imaging techniques,[116] capable of directly probing subpopulations of molecules in discrete transient states of dynamic processes (typically unresolvable in ensemble averages), will help track and therefore potentially elucidate mechanisms behind the dynamic behaviors of HP in biological activities. Availability of in-depth understanding of fundamental HP processes and profiles would further promote HP-based applications relevant for engineering specific genome modifications, altering spatial arrangements of chromosome domains, coordinating transcriptional activity, and constraining the outcome of DNA repair events. Finally, recent advances in single-molecule detection[117,118] can also be adapted to identify homology-dependent interactions between two half-PX DNA segments sliding in opposite directions.

## AUTHOR INFORMATION

### Corresponding Authors

*(X.W.) E-mail wangx28@rpi.edu.
*(A.R.C.) E-mail arunrichard@nyu.edu.
*(N.C.S.) E-mail ncs1@nyu.edu.

### ORCID

Xing Wang: 0000-0001-9930-3287
Arun Richard Chandrasekaran: 0000-0001-6757-5464



DOI: 10.1021/acs.chemrev.8b00207
Chem. Rev. XXXX, XXX, XXX−XXX

Megan E. Kizer: 0000-0003-3549-8606
Chengde Mao: 0000-0001-7516-8666
Hao Yan: 0000-0001-7397-9852
Baoquan Ding: 0000-0003-1095-8872

## Author Contributions

X.W. and A.R.C. initiated this discussion and designed the paper. X.W., A.R.C.. and N.C.S. wrote the manuscript. All authors provided comments on the manuscript and contributed to the original work discussed herein. X.W. and A.R.C. contributed equally.

## Funding

N.C.S. appreciates the following grants: EFRI-1332411 and CCF-1526650 from the NSF, MURI W911NF-11-1-0024 from the U.S. Army Research Office (ARO), N000141110729 from the U.S. Office of Naval Research (ONR), DE-SC0007991 from the U.S. Department of Energy (DOE) for DNA synthesis, and partial salary support and Grant GBMF3849 from the Gordon and Betty Moore Foundation. X.W. thanks Rensselaer Polytechnic Institute for new faculty start-up funds, RPI-CBIS Facility Award, and HT Materials gift funds.

## Notes

The authors declare no competing financial interest.

## Biographies

Xing Wang is an assistant professor in the Department of Chemistry and Chemical Biology and the Center for Biotechnology and Interdisciplinary Studies, Rensselaer Polytechnic Institute. He received a Ph.D. in chemistry from New York University (2009). After postdoctoral training at Princeton University exploring the novel functions of noncoding RNAs, he joined the faculty of Rensselaer in 2014. His research group is currently focused on the creation of designer DNA (origami) nanostructure-templated biological/bioinspired composites (including their applications in biology and medicine) and the development of RNA/DNA aptamer-based biosensors.

Arun Richard Chandrasekaran is a senior scientist at Confer Health, Inc. He received an M.Tech. in nanoscience from the University of Madras, India, in 2009 and a Ph.D. in chemistry from New York University in 2015. He did his postdoctoral research at The RNA Institute, University at Albany, State University of New York, where he worked on DNA nanoswitches for biomolecular detection and DNA-based nanostructures. He joined Confer Health, Inc., in 2016, and his current research focuses on developing clinical-grade diagnostics for home use.

Zhiyong Shen completed his doctoral degree in chemistry at New York University. Currently he is a professor in the College of Chemistry and Materials Science, Anhui Normal University, China. Before his current position, he served as a research scientist at Amersham Pharmacia Biotech, Genospectra, and Hologic Corp.

Yoel P. Ohayon is a professor in the Department of Chemistry, New York University. He received a B.A. in biochemistry from New York University (2000), M.Phil. in chemistry from New York University (2008), and Ph.D. in chemistry from New York University (2010). He joined the faculty of New York University in 2011. His research interests include DNA topology and self-assembled 3D DNA crystals.

Tong Wang received a B.S. in chemistry in 2000 from Shandong University, China, and completed his doctoral degree in chemistry in 2007 at New York University. After finishing his postdoctoral training at Brookhaven National Laboratory, he joined the Advanced Science Research Center (ASRC), Graduate Center of the City University of New York (CUNY), as an Imaging Facility manager and research assistant professor. His current research interests include molecular imaging by cryo-EM and 3D structural analysis of large biological molecular machines and DNA-based functional nanomaterials.

Megan E. Kizer is a Ph.D. candidate in the Department of Chemistry and Chemical Biology, Rensselaer Polytechnic Institute. She received a B.S. in 2015 from Binghamton University, where she studied protein−protein interactions of nuclear pore proteins in the laboratory of Sozanne Solmaz. Her current research is focused on investigating biotechnological applications of DNA nanostructures and RNA aptamers under the advisement of Drs. Xing Wang and Robert Linhardt.

Ruojie Sha is a senior research scientist in the Department of Chemistry, New York University. He received a B.S. in chemistry from Beijing University, Ph.D. in chemistry from New York University, and postdoctoral training at National Institutes of Health.

Chengde Mao is a professor in the Department of Chemistry, Purdue University. He received a B.S. in chemistry from Beijing University (1986) and Ph.D. in chemistry from New York University (1999). After postdoctoral training at Harvard University, he joined the faculty of Purdue University in 2002. His current research interest includes programmed DNA self-assembly and its applications.

Hao Yan received a B.S. degree in chemistry from Shandong University and Ph.D. degree in chemistry from New York University. He is currently the Milton D. Glick Distinguished Professor in the School of Molecular Sciences and the Biodesign Institute, Arizona State University (ASU). He directs the Biodesign Center for Molecular Design and Biomimetics at ASU.

Xiaoping Zhang received a B.S. in chemistry from Shandong University (1995) and Ph.D. in chemistry from New York University (2005). After postdoctoral training at New York University, in 2006, he joined Barr Lab Pharmaceuticals (now Teva Pharmaceutical Industries Ltd.) in 2008. Currently he is a principal scientist at Teva Pharmaceutical Industries Ltd.

Shiping Liao received a B.S. in polymer science from Beijing University of Chemical Technology (1995) and Ph.D. in chemistry from New York University (2005). He then joined the Barr Laboratory in 2006. Currently he is a scientist in AR&D at Teva Pharmaceuticals, developing validation analytical methods for generic drugs and preparing documents for ANDA filings.

Baoquan Ding received a B.S. in chemistry from Jilin University (2000) and Ph.D. in chemistry from New York University (2006). After postdoctoral training at Lawrence Berkeley National Laboratory, he joined the faculty of National Center for Nanoscience and Technology, China (NCNST), in 2010. His current research interests include functionalization of DNA-based assemblies and their applications.

Banani Chakraborty received a B.Sc. in chemistry from Calcutta University, India (2000), M.Sc. in chemistry from Indian Institute of Technology, Kanpur, India (2002), and Ph.D. in biomolecular chemistry from New York University (2008). She has done postdoctoral research at Simon Fraser University, Burnaby, Canada (2008−2011) and was an Alexander von Humboldt postdoctoral fellow in Rheinisch-Westfälische Technische Hochschule Aachen, Germany (2011−2014). She has been a DBT Ramalingaswami Fellow in the Department of Chemical Engineering, Indian Institute of Science, Bangalore, India, since 2015. Her research interests include application of DNA origami to merge top-down and bottom up DNA nanotechnology.



DOI: 10.1021/acs.chemrev.8b00207
Chem. Rev. XXXX, XXX, XXX−XXX

Natasha Jonoska is a professor in the Department of Mathematics and Statistics, University of South Florida. She received a dual B.S. in mathematics and computer science from University "Cyril and Methodius" in Skopje, Macedonia, and a Ph.D. in Mathematical Science from State University of New York, Binghamton. Her research interests include theoretical models for biomolecular information processing and DNA self-assembly.

Dong Niu received a Ph.D. in chemistry from New York University in 2015 for his dissertation on Structural Character and Formation Kinetics of Parametric Crossover DNA. His broad research interests include applied mathematical modeling, programmable molecular self-assembly, and structural DNA nanotechnology.

Hongzhou Gu obtained a Ph.D. in chemistry from New York University in 2010 and then worked as a postdoctoral researcher in molecular biology at Yale University. Currently he is a professor in the Institutes of Biomedical Sciences, Fudan University, China. His research focuses on the selection of aptamer-based sensors for molecular probing and imaging, as well as the development of smart DNA or RNA nanodevices for targeted drug delivery.

Jie Chao received a Ph.D. from Nanjing University in 2008. In 2006−2007, she was a visiting student in Professor Seeman's laboratory at New York University. After her postdoctoral research at Nanjing University, she joined the Shanghai Institute of Applied Physics (SINAP) in 2011 as an associate professor. In 2014, she moved to Nanjing University of Post & Telecommunications as a professor. Her research interests focus on DNA nanostructures and their biomedical applications.

Xiang Gao received a B.S. in biology from Shandong Univiersity (2009) and Ph.D in chemistry from New York University (2017). He is now a financial analyst of healthcare in Macquarie Securities Shanghai Office.

Yuhang Li received a B.S. in chemistry from the University of Science and Technology of China and Ph.D. in chemistry from New York University.

Tanashaya Ciengshin received a B.S. in biochemistry from Chulalongkorn University (2005) and Ph.D. in chemistry from New York University (2010). Currently she is a senior researcher at L'Oreal. Her current research interests are focused on new formulations and product development for hair and scalp.

Nadrian C. Seeman was born in Chicago in 1945. Following a B.S. in biochemistry from the University of Chicago, he received a Ph.D. in biological crystallography from the University of Pittsburgh in 1970. His postdoctoral training, at Columbia and Massachusetts Institute of Technology, emphasized nucleic acid crystallography. He was the first to demonstrate the correctness of Watson−Crick A-U base pairing at atomic resolution. He obtained his first independent position at State University of New York, Albany. Since 1988 he has worked at New York University, where he is the Margaret and Herman Sokol Professor of Chemistry. He was the founding president of the International Society for Nanoscale Science, Computation, and Engineering. He has published over 300 papers and has won the Sidhu Award, Feynman Prize, Emerging Technologies Award, Rozenberg Tulip Award in DNA Computing, World Technology Network Award in Biotechnology, NYACS Nichols Medal, SCC Frontiers of Science Award, ISNSCE Nanoscience Prize, Kavli Prize in Nanoscience, Einstein Professorship of the Chinese Academy of Sciences, Distinguished Alumnus Award from the University of Pittsburgh, Jagadish Chandra Bose Triennial Gold Medal, and Benjamin Franklin Medal in Chemistry. He received a Prose Award in Biological Sciences for his 2016 book, *Structural DNA Nanotechnology*, written during a John Simon Guggenheim Fellowship. He is a Thomson-Reuters Citation Laureate; has been elected a fellow of the American Association for the Advancement of Science, Royal Society of Chemistry, and American Crystallographic Association; and has been inducted as a fellow into the American Academy of Arts and Sciences.

## ABBREVIATIONS

| | |
|---|---|
| 1D | one-dimensional |
| 2D | two-dimensional |
| 6DF | six-domain flat |
| AFM | atomic force microscopy |
| AuNPs | gold nanoparticles |
| DX | double crossover |
| EM | electron microscopy |
| HJ | Holliday junction |
| HP | homologous pairing |
| HR | homologous recombination |
| LC−MS | liquid chromatography−mass spectrometry |
| MD | molecular dynamics |
| PCR | polymerase chain reaction |
| PX-DNA | paranemic crossover DNA |
| RCA | rolling-circle amplification |
| RIHP | recombination-independent homologous pairing |
| TEM | transmission electron microscopy |
| TPX | three-helical paranemic crossover |
| TX | triple crossover |
| XFEL | X-ray free electron laser |

## REFERENCES

(1) Seeman, N. C. Nucleic Acid Junctions and Lattices. *J. Theor. Biol.* **1982**, *99*, 237−247.
(2) Jones, M. R.; Seeman, N. C.; Mirkin, C. A. Programmable Materials and the Nature of the DNA Bond. *Science* **2015**, *347*, No. 1260901.
(3) Seeman, N. C. *Structural DNA Nanotechnology*, 1st ed.; Cambridge University Press: 2016.
(4) Shen, Z.; Yan, H.; Wang, T.; Seeman, N. C. Paranemic Crossover DNA: A Generalized Holliday Structure with Applications in Nanotechnology. *J. Am. Chem. Soc.* **2004**, *126*, 1666−1674.
(5) Yan, H.; Zhang, X.; Shen, Z.; Seeman, N. C. A Robust DNA Mechanical Device Controlled by Hybridization Topology. *Nature* **2002**, *415*, 62−65.
(6) Liao, S.; Seeman, N. C. Translation of DNA Signals into Polymer Assembly Instructions. *Science* **2004**, *306*, 2072−2074.
(7) Ding, B.; Seeman, N. C. Operation of a DNA Robot Arm Inserted into a 2D DNA Crystalline Substrate. *Science* **2006**, *314*, 1583−1585.
(8) Zhong, H.; Seeman, N. C. RNA Used to Control a DNA Rotary Nanomachine. *Nano Lett.* **2006**, *6*, 2899−2903.
(9) Chakraborty, B.; Sha, R.; Seeman, N. C. A DNA-Based Nanomechanical Device with Three Robust States. *Proc. Natl. Acad. Sci. U. S. A.* **2008**, *105*, 17245−17249.
(10) Gu, H.; Chao, J.; Xiao, S. J.; Seeman, N. C. Dynamic Patterning Programmed by DNA Tiles Captured on a DNA Origami Substrate. *Nat. Nanotechnol.* **2009**, *4*, 245−248.
(11) Liu, C.; Jonoska, N.; Seeman, N. C. Reciprocal DNA Nanomechanical Devices Controlled by the Same Set Strands. *Nano Lett.* **2009**, *9*, 2641−2647.
(12) Gu, H.; Chao, J.; Xiao, S. J.; Seeman, N. C. A Proximity-Based Programmable DNA Nanoscale Assembly Line. *Nature* **2010**, *465*, 202−205.
(13) Chakraborty, B.; Jonoska, N.; Seeman, N. C. A Programmable Transducer Self-Assembled from DNA. *Chem. Sci.* **2012**, *3*, 168−176.
(14) Jonoska, N.; Seeman, N. C. Computing by molecular self-assembly. *Interface Focus* **2012**, *2*, 504−511.


DOI: 10.1021/acs.chemrev.8b00207
*Chem. Rev.* XXXX, XXX, XXX−XXX

(15) Shih, W. M.; Quispe, J. D.; Joyce, G. F. A 1.7-Kilobase Single-Stranded DNA That Folds into a Nanoscale Octahedron. *Nature* **2004**, *427*, 618−621.
(16) Constantinou, P. E.; Wang, T.; Kopatsch, J.; Israel, L. B.; Zhang, X. P.; Ding, B. Q.; Sherman, W. B.; Wang, X.; Zheng, J. P.; Sha, R. J.; Seeman, N. C. Double Cohesion in Structural DNA Nanotechnology. *Org. Biomol. Chem.* **2006**, *4*, 3414−3419.
(17) Liu, W. Y.; Wang, X.; Wang, T.; Sha, R. J.; Seeman, N. C. PX DNA Triangle Oligomerized Using a Novel Three-Domain Motif. *Nano Lett.* **2008**, *8*, 317−322.
(18) Ohayon, Y. R.; Sha, R. J.; Flint, O.; Liu, W. Y.; Chakraborty, B.; Subramanian, H. K. K.; Zheng, J. P.; Chandrasekaran, A. R.; Abdallah, H. O.; Wang, X.; Zhang, X. P.; Seeman, N. C. Covalent Linkage of One-Dimensional DNA Arrays Bonded by Paranemic Cohesion. *ACS Nano* **2015**, *9*, 10304−10312.
(19) Ohayon, Y. P.; Sha, R. J.; Flint, O.; Chandrasekaran, A. R.; Abdallah, H. O.; Wang, T.; Wang, X.; Zhang, X. P.; Seeman, N. C. Topological Linkage of DNA Tiles Bonded by Paranemic Cohesion. *ACS Nano* **2015**, *9*, 10296−10303.
(20) Shen, W. L.; Liu, Q.; Ding, B. Q.; Shen, Z. Y.; Zhu, C. Q.; Mao, C. D. The Study Of the Paranemic Crossover (PX) Motif in the Context of Self-Assembly of DNA 2D Crystals. *Org. Biomol. Chem.* **2016**, *14*, 7187−7190.
(21) Shen, W. L.; Liu, Q.; Ding, B.; Zhu, C. Q.; Shen, Z.; Seeman, N. C. Facilitation of DNA Self-Assembly by Relieving the Torsional Strains between Building Blocks. *Org. Biomol. Chem.* **2017**, *15*, 465−469.
(22) Lin, C.; Wang, X.; Liu, Y.; Seeman, N. C.; Yan, H. Rolling Circle Enzymatic Replication of a Complex Multi-Crossover DNA Nanostructure. *J. Am. Chem. Soc.* **2007**, *129*, 14475−14481.
(23) Lin, C.; Rinker, S.; Wang, X.; Liu, Y.; Seeman, N. C.; Yan, H. In Vivo Cloning of Artificial DNA Nanostructures. *Proc. Natl. Acad. Sci. U. S. A.* **2008**, *105*, 17626−17631.
(24) Wang, X.; Zhang, X.; Mao, C.; Seeman, N. C. Double-Stranded DNA Homology Produces a Physical Signature. *Proc. Natl. Acad. Sci. U. S. A.* **2010**, *107*, 12547−12552.
(25) Holliday, R. A Mechanism for Gene Conversion in Fungi. *Genet. Res.* **1964**, *5*, 282−304.
(26) Kallenbach, N. R.; Ma, R. I.; Seeman, N. C. An Immobile Nucleic-Acid Junction Constructed from Oligonucleotides. *Nature* **1983**, *305*, 829−831.
(27) Ma, R. I.; Kallenbach, N. R.; Sheardy, R. D.; Petrillo, M. L.; Seeman, N. C. Three-Arm Nucleic Acid Junctions are Flexible. *Nucleic Acids Res.* **1986**, *14*, 9745−9753.
(28) Wang, Y.; Mueller, J. E.; Kemper, B.; Seeman, N. C. Assembly and Characterization of Five-Arm and Six-Arm DNA Branched Junctions. *Biochemistry* **1991**, *30*, 5667−5674.
(29) Wang, X.; Seeman, N. C. Assembly and Characterization of 8-Arm and 12-Arm DNA Branched Junctions. *J. Am. Chem. Soc.* **2007**, *129*, 8169−8176.
(30) Fu, T.-J.; Seeman, N. C. DNA Double-Crossover Molecules. *Biochemistry* **1993**, *32*, 3211−3220.
(31) LaBean, T.; Yan, H.; Kopatsch, J.; Liu, F.; Winfree, E.; Reif, J. H.; Seeman, N. C. Construction, Analysis, Ligation, and Self-Assembly of DNA Triple Crossover Complexes. *J. Am. Chem. Soc.* **2000**, *122*, 1848−1860.
(32) Winfree, E.; Liu, F. R.; Wenzler, L. A.; Seeman, N. C. Design and Self-Assembly of Two-Dimensional DNA Crystals. *Nature* **1998**, *394*, 539−544.
(33) Pinto, Y. Y.; Le, J. D.; Seeman, N. C.; Musier-Forsyth, K.; Taton, T. A.; Kiehl, R. A. Sequence-Encoded Self-Assembly of Multiple-Nanocomponent Arrays by 2D DNA Scaffolding. *Nano Lett.* **2005**, *5*, 2399−2402.
(34) Williams, B. A.; Lund, K.; Liu, Y.; Yan, H.; Chaput, J. C. Self-Assembled Peptide Nanoarrays: An Approach to Studying Protein-Protein Interactions. *Angew. Chem., Int. Ed.* **2007**, *46*, 3051−3054.
(35) Maiti, P. K.; Pascal, T. A.; Vaidehi, N.; Heo, J.; Goddard, W. A., 3rd Atomic-Level Simulations of Seeman DNA Nanostructures: The Paranemic Crossover in Salt Solution. *Biophys. J.* **2006**, *90*, 1463−1479.
(36) McGavin, S. Models of Specifically Paired Like (Homologous) Nucleic Acid Structures. *J. Mol. Biol.* **1971**, *55*, 293−298.
(37) Wilson, J. H. Nick-Free Formation of Reciprocal Hetero-duplexes: A Simple Solution to the Topological Problem. *Proc. Natl. Acad. Sci. U. S. A.* **1979**, *76*, 3641−3645.
(38) Bhatia, D.; Mehtab, S.; Krishnan, R.; Indi, S. S.; Basu, A.; Krishnan, Y. Icosahedral DNA Nanocapsules by Modular Assembly. *Angew. Chem., Int. Ed.* **2009**, *48*, 4134−4137.
(39) Yang, X. P.; Wenzler, L. A.; Qi, J.; Li, X. J.; Seeman, N. C. Ligation of DNA Triangles Containing Double Crossover Molecules. *J. Am. Chem. Soc.* **1998**, *120*, 9779−9786.
(40) Zhang, X.; Yan, H.; Shen, Z.; Seeman, N. C. Paranemic Cohesion of Topologically-Closed DNA Molecules. *J. Am. Chem. Soc.* **2002**, *124*, 12940−12941.
(41) Viasnoff, V.; Meller, A.; Isambert, H. DNA Nanomechanical Switches under Folding Kinetics Control. *Nano Lett.* **2006**, *6*, 101−104.
(42) Tashiro, R.; Sugiyama, H. A Nanothermometer Based on the Different $\pi$ Stackings of B- and Z-DNA. *Angew. Chem., Int. Ed.* **2003**, *42*, 6018−6020.
(43) Idili, A.; Vallee-Belisle, A.; Ricci, F. Programmable pH-Triggered DNA Nanoswitches. *J. Am. Chem. Soc.* **2014**, *136*, 5836−5839.
(44) Saha, S.; Prakash, V.; Halder, S.; Chakraborty, K.; Krishnan, Y. A pH-Independent DNA Nanodevice for Quantifying Chloride Transport in Organelles of Living Cells. *Nat. Nanotechnol.* **2015**, *10*, 645−651.
(45) Mao, C. D.; Sun, W. Q.; Shen, Z. Y.; Seeman, N. C. A Nanomechanical Device Based on the B-Z Transition of DNA. *Nature* **1999**, *397*, 144−146.
(46) Miduturu, C. V.; Silverman, S. K. DNA Constraints Allow Rational Control of Macromolecular Conformation. *J. Am. Chem. Soc.* **2005**, *127*, 10144−10145.
(47) Liang, X.; Nishioka, H.; Takenaka, N.; Asanuma, H. A DNA Nanomachine Powered by Light Irradiation. *ChemBioChem* **2008**, *9*, 702−705.
(48) Uno, S. N.; Dohno, C.; Bittermann, H.; Malinovskii, V. L.; Haner, R.; Nakatani, K. A Light-Driven Supramolecular Optical Switch. *Angew. Chem., Int. Ed.* **2009**, *48*, 7362−7365.
(49) Shen, W. Q.; Bruist, M. F.; Goodman, S. D.; Seeman, N. C. A Protein-Driven DNA Device That Measures the Excess Binding Energy of Proteins That Distort DNA. *Angew. Chem., Int. Ed.* **2004**, *43*, 4750−4752.
(50) Gu, H. Z.; Yang, W.; Seeman, N. C. DNA Scissors Device Used to Measure MutS Binding to DNA Mis-pairs. *J. Am. Chem. Soc.* **2010**, *132*, 4352−4357.
(51) Yurke, B.; Turberfield, A. J.; Mills, A. P.; Simmel, F. C.; Neumann, J. L. A DNA-Fuelled Molecular Machine Made of DNA. *Nature* **2000**, *406*, 605−608.
(52) Rothemund, P. W. Folding DNA to Create Nanoscale Shapes and Patterns. *Nature* **2006**, *440*, 297−302.
(53) Liu, D.; Wang, M. S.; Deng, Z. X.; Walulu, R.; Mao, C. D. Tensegrity: Construction of Rigid DNA Triangles with Flexible Four-Arm DNA Junctions. *J. Am. Chem. Soc.* **2004**, *126*, 2324−2325.
(54) Li, Y. *Programmable Molecular Choreography in a DNA Transducer Produced by Self-Assembly*. Ph.D. Thesis 3635349; New York University, 2014; https://pqdtopen.proquest.com/doc/1615130290.html?FMT=ABS.
(55) Ackermann, D.; Jester, S. S.; Famulok, M. Design Strategy for DNA Rotaxanes with a Mechanically Reinforced PX100 Axle. *Angew. Chem., Int. Ed.* **2012**, *51*, 6771−6775.
(56) Ackermann, D.; Schmidt, T. L.; Hannam, J. S.; Purohit, C. S.; Heckel, A.; Famulok, M. A Double-Stranded DNA Rotaxane. *Nat. Nanotechnol.* **2010**, *5*, 436−442.
(57) Chen, J. H.; Seeman, N. C. Synthesis From DNA of a Molecule with the Connectivity of a Cube. *Nature* **1991**, *350*, 631−633.


DOI: 10.1021/acs.chemrev.8b00207
*Chem. Rev.* XXXX, XXX, XXX−XXX

(58) Zhang, C.; Ko, S. H.; Su, M.; Leng, Y. J.; Ribbe, A. E.; Jiang, W.; Mao, C. D. Symmetry Controls the Face Geometry of DNA Polyhedra. *J. Am. Chem. Soc.* **2009**, *131*, 1413−1415.
(59) He, Y.; Ye, T.; Su, M.; Zhang, C.; Ribbe, A. E.; Jiang, W.; Mao, C. D. Hierarchical Self-Assembly of DNA into Symmetric Supramolecular Polyhedra. *Nature* **2008**, *452*, 198−U141.
(60) Zhang, Y. W.; Seeman, N. C. Construction of a DNA-Truncated Octahedron. *J. Am. Chem. Soc.* **1994**, *116*, 1661−1669.
(61) He, Y.; Su, M.; Fang, P. A.; Zhang, C.; Ribbe, A. E.; Jiang, W.; Mao, C. D. On the Chirality of Self-Assembled DNA Octahedra. *Angew. Chem., Int. Ed.* **2010**, *49*, 748−751.
(62) Shen, Z. *DNA Poly-Crossover Molecules and Their Applications in Homology Recognition*; Ph.D. Thesis, New York University, 1999.
(63) Zhang, F.; Jiang, S. X.; Wu, S. Y.; Li, Y. L.; Mao, C. D.; Liu, Y.; Yan, H. Complex Wireframe DNA Origami Nanostructures with Multi-Arm Junction Vertices. *Nat. Nanotechnol.* **2015**, *10*, 779−784.
(64) Benson, E.; Mohammed, A.; Gardell, J.; Masich, S.; Czeizler, E.; Orponen, P.; Hogberg, B. DNA Rendering of Polyhedral Meshes at the Nanoscale. *Nature* **2015**, *523*, 441−444.
(65) Veneziano, R.; Ratanalert, S.; Zhang, K.; Zhang, F.; Yan, H.; Chiu, W.; Bathe, M. Designer Nanoscale DNA Assemblies Programmed from the Top Down. *Science* **2016**, *352*, 1534.
(66) Han, D.; Qi, X.; Myhrvold, C.; Wang, B.; Dai, M.; Jiang, S.; Bates, M.; Liu, Y.; An, B.; Zhang, F.; Yan, H.; Yin, P. Single-Stranded DNA and RNA Origami. *Science* **2017**, *358*, No. eaao2648.
(67) Li, Z.; Wei, B.; Nangreave, J.; Lin, C.; Liu, Y.; Mi, Y.; Yan, H. A Replicable Tetrahedral Nanostructure Self-Assembled from a Single DNA Strand. *J. Am. Chem. Soc.* **2009**, *131*, 13093−13098.
(68) Lin, C.; Xie, M.; Chen, J. J.; Liu, Y.; Yan, H. Rolling-Circle Amplification of a DNA Nanojunction. *Angew. Chem., Int. Ed.* **2006**, *45*, 7537−7539.
(69) Geary, C.; Rothemund, P. W.; Andersen, E. S. RNA Nanostructures. A Single-Stranded Architecture for Cotranscriptional Folding of RNA Nanostructures. *Science* **2014**, *345*, 799−804.
(70) Rankin, S.; Flint, O.; Schermann, J. Enumerating the Prime Alternating Knots, Part I. *J. Knot Theory Ramifications* **2004**, *13*, 57−100.
(71) Rankin, S.; Flint, O.; Schermann, J. Enumerating the Prime Alternating Knots, Part II. *J. Knot Theory Ramifications* **2004**, *13*, 101−149.
(72) Ding, B. Q.; Sha, R. J.; Seeman, N. C. Pseudohexagonal 2D DNA Crystals from Double Crossover Cohesion. *J. Am. Chem. Soc.* **2004**, *126*, 10230−10231.
(73) Qiu, H.; Dewan, J. C.; Seeman, N. C. A DNA Decamer with a Sticky End: The Crystal Structure of d-CGACGATCGT. *J. Mol. Biol.* **1997**, *267*, 881−898.
(74) Kosuri, S.; Church, G. M. Large-Scale De Novo DNA Synthesis: Technologies and Applications. *Nat. Methods* **2014**, *11*, 499−507.
(75) Ma, Y.; Zheng, H.; Wang, C.; Yan, Q.; Chao, J.; Fan, C.; Xiao, S. J. RCA Strands as Scaffolds to Create Nanoscale Shapes by a Few Staple Strands. *J. Am. Chem. Soc.* **2013**, *135*, 2959−2962.
(76) Ouyang, X.; Li, J.; Liu, H.; Zhao, B.; Yan, J.; Ma, Y.; Xiao, S.; Song, S.; Huang, Q.; Chao, J.; Fan, C. Rolling Circle Amplification-Based DNA Origami Nanostructrures for Intracellular Delivery of Immunostimulatory Drugs. *Small* **2013**, *9*, 3082−3087.
(77) Sambrook, J.; Russell, D. *Molecular Cloning: A Laboratory Manual*, 3rd ed.; Cold Spring Harbor Laboratory Press: Cold Spring Harbor, NY, 2001.
(78) Veneziano, R.; Shepherd, T. R.; Ratanalert, S.; Bellou, L.; Tao, C.; Bathe, M. In Vitro Synthesis of Gene-Length Single-Stranded DNA. *Sci. Rep.* **2018**, *8*, No. 6548.
(79) Barzel, A.; Kupiec, M. Finding a Match: How Do Homologous Sequences Get Together for Recombination? *Nat. Rev. Genet.* **2008**, *9*, 27−37.
(80) Apte, M. S.; Meller, V. H. Homologue Pairing in Flies and Mammals: Gene Regulation When Two are Involved. *Genet. Res. Int.* **2012**, *2012*, No. 430587.
(81) Joyce, E. F.; Apostolopoulos, N.; Beliveau, B. J.; Wu, C. T. Germline Progenitors Escape the Widespread Phenomenon of Homolog Pairing During Drosophila Development. *PLoS Genet.* **2013**, *9*, No. e1004013.
(82) Hassold, T.; Hunt, P. To ERR (Meiotically) is Human: The Genesis of Human Aneuploidy. *Nat. Rev. Genet.* **2001**, *2*, 280−291.
(83) Strick, T. R.; Croquette, V.; Bensimon, D. Homologous Pairing in Stretched Supercoiled DNA. *Proc. Natl. Acad. Sci. U. S. A.* **1998**, *95*, 10579−10583.
(84) Nishikawa, J.-I.; Ohyama, T. Selective Association between Nucleosomes with Identical DNA Sequences. *Nucleic Acids Res.* **2013**, *41*, 1544−1554.
(85) Conley, E. C.; West, S. C. Homologous Pairing and the Formation of Nascent Synaptic Intermediates between Regions of Duplex DNA by RecA Protein. *Cell* **1989**, *56*, 987−995.
(86) Vologodskii, A. V.; Lukashin, A. V.; Anshelevich, V. V.; Frankkamenetskii, M. D. Fluctuations in Superhelical DNA. *Nucleic Acids Res.* **1979**, *6*, 967−982.
(87) Gilbert, N.; Allan, J. Supercoiling in DNA and Chromatin. *Curr. Opin. Genet. Dev.* **2014**, *25*, 15−21.
(88) Kleckner, N. Questions and Assays. *Genetics* **2016**, *204*, 1343−1349.
(89) Santosh, M.; Maiti, P. K. Structural Rigidity of Paranemic Crossover and Juxtapose DNA. *Biophys. J.* **2011**, *101*, 1393−1402.
(90) Maiti, P. K.; Pascal, T. A.; Vaidehi, N.; Goddard, W. A., III The Stability of Seeman JX DNA Topoisomers of Paranemic Crossover (PX) Molecules as a Function of Crossover Number. *Nucleic Acids Res.* **2004**, *32*, 6047−6056.
(91) Wang, T. *Structural DNA Nanotechnology: Design and Self Assembly of 2D and 3D Crystalline Lattices*; Ph.D. Thesis, New York University, 2007.
(92) Zheng, J. P.; Birktoft, J. J.; Chen, Y.; Wang, T.; Sha, R. J.; Constantinou, P. E.; Ginell, S. L.; Mao, C. D.; Seeman, N. C. From Molecular to Macroscopic via the Rational Design of a Self-Assembled 3D DNA Crystal. *Nature* **2009**, *461*, 74−77.
(93) Ke, Y.; Ong, L. L.; Sun, W.; Song, J.; Dong, M.; Shih, W. M.; Yin, P. DNA Brick Crystals with Prescribed Depths. *Nat. Chem.* **2014**, *6*, 994−1002.
(94) Martin, T. G.; Bharat, T. A.; Joerger, A. C.; Bai, X. C.; Praetorius, F.; Fersht, A. R.; Dietz, H.; Scheres, S. H. Design of a Molecular Support for Cryo-EM Structure Determination. *Proc. Natl. Acad. Sci. U. S. A.* **2016**, *113*, E7456−E7463.
(95) Chapman, H. N. Structure Determination Using X-Ray Free-Electron Laser Pulses. *Methods Mol. Biol.* **2017**, *1607*, 295−324.
(96) Kuhlbrandt, W. Cryo-EM Enters a New Era. *eLife* **2014**, *3*, No. e03678.
(97) Georgiadis, M. M.; Singh, I.; Kellett, W. F.; Hoshika, S.; Benner, S. A.; Richards, N. G. Structural Basis for a Six Nucleotide Genetic Alphabet. *J. Am. Chem. Soc.* **2015**, *137*, 6947−6955.
(98) Malyshev, D. A.; Dhami, K.; Lavergne, T.; Chen, T.; Dai, N.; Foster, J. M.; Correa, I. R., Jr.; Romesberg, F. E. A Semi-Synthetic Organism with an Expanded Genetic Alphabet. *Nature* **2014**, *509*, 385−388.
(99) Taylor, A. I.; Beuron, F.; Peak-Chew, S. Y.; Morris, E. P.; Herdewijn, P.; Holliger, P. Nanostructures from Synthetic Genetic Polymers. *ChemBioChem* **2016**, *17*, 1107−1110.
(100) He, Y. F.; Li, B. Z.; Li, Z.; Liu, P.; Wang, Y.; Tang, Q.; Ding, J.; Jia, Y.; Chen, Z.; Li, L.; Sun, Y.; Li, X.; Dai, Q.; Song, C. X.; Zhang, K.; He, C.; Xu, G. L. Tet-Mediated Formation of 5-Carboxylcytosine and Its Excision by TDG in Mammalian DNA. *Science* **2011**, *333*, 1303−1307.
(101) Liu, Q.; Liu, G.; Wang, T.; Fu, J.; Li, R.; Song, L.; Wang, Z. G.; Ding, B.; Chen, F. Enhanced Stability of DNA Nanostructures by Incorporation of Unnatural Base Pairs (UBPs). *ChemPhysChem* **2017**, *18* (21), No. 2977.
(102) Chen, Y.; Mao, C. Reprogramming DNA-Directed Reactions on the Basis of a DNA Conformational Change. *J. Am. Chem. Soc.* **2004**, *126*, 13240−13241.


DOI: 10.1021/acs.chemrev.8b00207
*Chem. Rev.* XXXX, XXX, XXX−XXX

(103) Marchi, A. N.; Saaem, I.; Vogen, B. N.; Brown, S.; LaBean, T. H. Toward Larger DNA Origami. *Nano Lett.* **2014**, *14*, 5740−5747.
(104) Subramanian, H. K. K.; Chakraborty, B.; Sha, R.; Seeman, N. C. The Label-Free Unambiguous Detection and Symbolic Display of Single Nucleotide Polymorphisms on DNA Origami. *Nano Lett.* **2011**, *11*, 910−913.
(105) Pang, S.; Liu, S. Y.; Su, X. G. A Fluorescence Assay for the Trace Detection of Protamine and Heparin. *RSC Adv.* **2014**, *4*, 25857−25862.
(106) Afonin, K. A.; Cieply, D. J.; Leontis, N. B. Specific RNA Self-Assembly with Minimal Paranemic Motifs. *J. Am. Chem. Soc.* **2008**, *130*, 93−102.
(107) Afonin, K. A.; Danilov, E. O.; Novikova, I. V.; Leontis, N. B. Tokenrna: A New Type of Sequence-Specific, Label-Free Fluorescent Biosensor for Folded RNA Molecules. *ChemBioChem* **2008**, *9*, 1902−1905.
(108) Sun, D.; Hurley, L. H. The Importance of Negative Superhelicity in Inducing the Formation of G-Quadruplex and i-Motif Structures in the c-Myc Promoter: Implications for Drug Targeting and Control of Gene Expression. *J. Med. Chem.* **2009**, *52*, 2863−2874.
(109) Tuerk, C.; Gold, L. Systematic Evolution of Ligands by Exponential Enrichment - RNA Ligands to Bacteriophage-T4 DNA-Polymerase. *Science* **1990**, *249*, 505−510.
(110) Darmostuk, M.; Rimpelova, S.; Gbelcova, H.; Ruml, T. Current Approaches in SELEX: An Update to Aptamer Selection Technology. *Biotechnol. Adv.* **2015**, *33*, 1141−1161.
(111) Packer, M. S.; Liu, D. R. Methods for the Directed Evolution of Proteins. *Nat. Rev. Genet.* **2015**, *16*, 379−394.
(112) Harlow, E.; Lane, D. *Using Antibodies: A Laboratory Manual*; Cold Spring Harbor Laboratory Press: Cold Spring Harbor, NY, 1999.
(113) Bennett, S. Solexa Ltd. *Pharmacogenomics* **2004**, *5*, 433−438.
(114) Aebersold, R.; Mann, M. Mass Spectrometry-Based Proteomics. *Nature* **2003**, *422*, 198−207.
(115) Domon, B.; Aebersold, R. Mass Spectrometry and Protein Analysis. *Science* **2006**, *312*, 212−217.
(116) Huang, B.; Babcock, H.; Zhuang, X. W. Breaking the Diffraction Barrier: Super-Resolution Imaging of Cells. *Cell* **2010**, *143*, 1047−1058.
(117) Liu, C.; Danilowicz, C.; Kleckner, N.; Prentiss, M. Single Molecule Identification of Homology-Dependent Interactions between Long ssrna and dsdna. *Nucleic Acids Res.* **2017**, *45*, 894−901.
(118) Danilowicz, C.; Lee, C. H.; Kim, K.; Hatch, K.; Coljee, V. W.; Kleckner, N.; Prentiss, M. Single Molecule Detection of Direct, Homologous, DNA/DNA Pairing. *Proc. Natl. Acad. Sci. U. S. A.* **2009**, *106*, 19824−19829.



DOI: 10.1021/acs.chemrev.8b00207
*Chem. Rev.* XXXX, XXX, XXX−XXX